EUROPEAN SOUTHERN OBSERVATORY

Organisation Européenne pour des Recherches Astronomiques dans l'Hémisphere Austral
Europäische Organisation für astronomische Forschung in der südlichen Hemisphäre

VERY LARGE TELESCOPE

PRIMA Metrology design description

Doc. No. VLT-TRE-ESO-15730-3000

Issue 2

Date 02/04/08

Prepared . . . .
S. Leveque
Name   Date   Signature

Approved . . . .
F.Delplancke
Name   Date   Signature

Released . . . .
R.Gilmozzi
Name   Date   Signature

Change Record

Issue / Rev.	Date	Section / Page. affected	Reason/Remarks
2	02/04/08	all	Issue for PAE

Table of Contents

1 Scope

This document presents the design the PRIMA Metrology System. It shall also be used an overview document, where the reader will be pointed to the appropriate reference document for design and implementation details.

2 Applicable Documents

AD 1   VLT-SPE-ESO-15730-2211, issue 1, October 2000, Technical Specifications for the PRIMA Metrology System

3 Reference Documents

RD 1   VLT-LIS-ESO-15730-2995, issue 2, 02/04/08, Configuration Item Data List for the PRIMA Metrology System

RD 2   VLT-PLA-ESO-15730-3175, issue 1, 26/04/08, Alignment Plan for the PRIMA Metrology System

RD 3   VLT-ICD-ESO-15730-2922, issue 3, 08/12/03, VLTI PRIMA Interface Control Document between the Metrology System and the AT Star Separator

RD 4   VLT-TRE-ESO-15730-4546, Issue 1, 02/04/08, PRIMA Metrology safety and reliability analysis

RD 5   VLT-TRE-ESO-15730-4042, Issue 1,02/04/08, Metrology Test Report

RD 6   VLT-TRE-IMT-15731-3154, Issue 4,19/12/03, Design of the Laser Assembly of the PRIMA Metrology System

RD 7   VLT-TRE-ESO-15731-3884, Issue 1, 26/6/06, Test of the laser frequency stabilization system of the PRIMA Metrology System

RD 8   VLT-SPE-ESO-15732-3799, issue 1, 5/7/2007, Specifications for high sensitive 4-quadrant detectors for the PRIMA Metrology System

RD 9   VLT-TRE-ESO-15732-4087, issue 1, 02/04/08, Design of the Pupil Tracker for PRIMET

RD 10   VLT-TRE-ESO-15732-4542, issue 1, Performance of the Metrology Pupil tracking measured on STS#AT1in Garching

RD 11   VLT-TRE-IMT-15374-3726, issue 1, 20/7/2005, As built Phase Meter configuration for the PRIMA Metrology System

RD 12   VLT-MAN-ESO-15734-4535, issue1, 17/3/08, Modifications of the phasemeter firmware

RD 13   VLT-TRE-ESO-15735-2963, issue 2, 03/04/08, PRIMA Metrology Control Electronics

RD 14   VLT-TRE-ESO-15735-4544,issue 1, 01/04/08, Design of the PRIMA Metrology Interlock System.

RD 15   VLT-TRE-ESO-15736-2998, issue 2, 29/04/2008, VLTI Software - PRIMA Metrology Control Software - Design Description

RD 16   VLT-SPE-ESO-15736-3899, issue 1, 02/04/2008, Specification for the PRIMA Metrology data files, data logging and algorithms

RD 17   VLT-TRE-ESO-15736-4544, issue 1, 02/04/2008, Operation scenario for PRIMET

RD 18   VLT-MAN-ESO-15736-4547, issue 1, 29/04/2008,PRIMA Metrology Software User Manual

4   Acronyms

- AIT: Assembly, Integration and Test
- AOM: Acousto-Optics Modulator
- AD: Applicable Document
- BC: Beam Combiner
- BS: Beam Splitter
- FDR: Final Design Review
- FSU: Fringe Sensor Unit
- FSU-BC: Fringe Sensor Unit Beam Combiner
- FTK: Fringe Tracking Testbed
- FWHM: Full Width Half Maximum
- HW: Hardware
- IMT: Institute of Microtechnology of Neuchatel
- KO: Kick Off
- NPRO:Non-Planar Ring Oscillator
- OPD: Optical Path Difference
- PBS: Polarization Beam Splitter
- PDR: Preliminary Design Review
- PM: Polarization Maintaining
- PSD: Position Sensitive Detector
- PRIMA:Phase Referenced Imaging and Micro-arcsec Astrometry
- RD:Reference Document
- RMN:Reflective Memory Network
- SHG:Second Harmonic Generation
- SM: Single Mode
- STS: Star Separator
- SW: Software
- TBC:To Be Confirmed
- TBD:To Be Defined

5   System Overview

The PRIMA Metrology System is a component of the PRIMA facility. This system ties together the two interferometric signals obtained by the simultaneous coherent observation of two celestial objects with PRIMA. The role of this Metrology System is to monitor the PRIMA instrumental optical path errors to ultimately reach a final instrumental phase accuracy limited by atmospheric piston anisoplanatism.

In order to place the metrology system in the context of PRIMA, two celestial objects of vector coordinates S_1 and S_2 are considered. These objects are simultaneously observed on two independent beam combiners (A and B), i.e using a dual-feed configuration. By stabilizing the interference fringes on the so-called bright object S_1, the residual Optical Path Difference, ΔOPD, seen by S_2 is given by:

$$\Delta OPD = B. (S_2 - S_1) + \phi/k + \delta A + \Delta L$$

where

- B is the vector baseline of the interferometer
- ϕ is a phase factor inherent to the nature of the observed objects and is the observable for phased-referenced imaging, k being the wave number.
- δA represents the differential OPD (or piston) anisoplanatism which contributes to the residual fringe motion seen by S_2. For the maximum angular separation $S_2 - S_1$ of PRIMA of 1 arcmin, the standard deviation of δA is about 2 μm rms, i.e. 10 times lower than the open-loop atmospheric fringe motion imposed on S_1. δA has a zero mean and can be averaged-out down to 5 nm rms by successive measurements of ΔOPD in a typical 30 min. time frame for a 10 arcsec star separation.
- $\Delta L = L_A - L_B$ represents the difference between the internal OPD's of each channel. DL can thus be seen as the instrumental contribution to ΔOPD.

Knowing the baseline vector B and by measuring independently ΔOPD and ΔL, Eq.(1) shows that one can estimate either the factor ϕ/k for a known star separation (Phase-referenced Imaging mode), or inversely the star separation for a known ϕ (Astrometric mode). The bottom line being that the implementation of PRIMA is intimately linked with the ability to trace back the "differential" internal OPD between the two objects, ΔL.

In the VLTI, the light captured by two telescopes follows a train of 25 mirrors distributed along a subterranean path of approximately 200 meters, before being coherently combined. Inside the VLTI, the fringe signals are affected by static optical path differences and also by time-varying optical path fluctuations introduced by the motion of the Delay lines and of the Differential Delay Lines, by vibrations of mechanical structures, and by air turbulence. The PRIMA Metrology system is designed to monitor these instrumental disturbances, which are included in the variable ΔL, with an ultimate accuracy goal of 5 nm, AD 1.

The concept of the PRIMA Metrology System is based on "super-heterodyne laser interferometry", where two heterodyne Michelson interferometers are operating simultaneously and have common optical paths with both observed stars through the VLTI optical train, i.e. from the interferometric laboratory to the metrology "end-points" (retro-reflectors) located inside the telescopes. The disturbance to be monitored, ΔL, corresponds to the difference between the path variations recorded by the two Michelson interferometers.

Because such a system is purely incremental (i.e. counting the number of 2π phase variation while ΔL is varying), the estimation of the absolute value of ΔL implies an accurate calibration of the metrology "zero" point, i.e. when $\Delta L = 0$. For this calibration, one solution consists in the simultaneous observation of the bright celestial object on both PRIMA channels, for which ΔL must be zero by definition ($S_2 = S_1$, $\delta A = 0$, $\phi = 0$ for a point-like bright object). Starting from this calibration mode, the metrology system is zeroed and ΔL is continuously monitored while S_2 is acquired and tracked on the Channel A of PRIMA. An alternative consists in "swapping" the objects, by feeding the beam combiner A with S_2 and the beam combiner B with S_1 and by recording the OPD to estimate the absolute value of ΔL (see example in appendix 15.1).

However in both cases, if internal OPD disturbances larger than $\lambda/2$ occur between the zero OPD calibration sequence and the start of the measurement or if the laser beams are suddenly lost or interrupted, a re-calibration is needed. In order to avoid this potentially time consuming sequence and to increase the overall robustness, an upgrade of PRIMET to an absolute metrology system could be implemented thanks to the commercial availability of frequency combs.

The current document addresses only on the incremental version of PRIMET.

Details about absolute metrology for PRIMA can be found in:

- " Frequency comb referenced two-wavelength source for absolute distance measurement ", N. Schuhler, Y. Salvadé, S. Lévêque, R. Dändliker, R. Holzwarth, Opt. Lett. 31, 3101-3103 (2006)

- "Absolute Metrology for the Very Large Telescope Interferometer ", Y. Salvadé, R. Dändliker, N. Schuhler, S. Lévêque, S. Le Floch, Conference ODIMAP V, Madrid, October 06.

- "High-accuracy absolute distance measurement using frequency comb referenced multi-wavelength source", Y. Salvadé, N.Schuhler, S.Lévêque and S.Le Floch, accepted for publication in Applied optics (April 2008)

The PRIMA Metrology system is a "sensor" which measures the quantity ΔL and write it on the Reflective Memory Network, as shown in Fig. 1. The Metrology sub-system breakdown is shown in Fig. 2.

Light Source:

This sub-system includes the laser head, the heterodyne assembly and its control HW/SW. Its role is to provide to the metrology system all necessary laser beams characterized by their wavelength, frequency stability, optical power, polarization state, and the relevant heterodyne frequencies. The light source sub-system and its associated electronics is located in the VLTI storage room. Its major component aim at stabilizing the laser frequency on an Iodine absorption line.

Beam launchers/Beam combiner:

The role of the beam launcher sub-system is to inject the laser beam(s) provided by the light source sub-system into each stellar channel, with the appropriate optical characteristics. The beam combiner is the location where the metrology beams of each channel interfere. As shown in Fig. 3, there will be one beam launcher/combiner on each of the following optical tables: FSU#A, FSU#B, AMBER and MIDI.

This sub-system include 4-quadrant detectors to sense the lateral displacement of the metrology beams after a round trip in the VLTI. Corrections will be sent the STS to maintain the metrology beams aligned during observations.

Metrology end-points (retro-reflectors)

The metrology end-points terminate the internal optical path monitored by the metrology system by retro-reflecting the metrology beams back to their injection points. For the Auxiliary Telescope the retro-reflector system is integrated inside the Star Separator.

For the UT's, the retro-reflector (same concept as for the AT-STS) will be located behind the M9 dichroic mirror, in the Coude room.

Phase meter

The role of the phase meter is to detect and process the metrology interference signals to retrieve the quantity ΔL and make it available to the PRIMA control system.

Control HW/SW

This sub-system includes the hardware and software required to control the metrology system and exchange data/status/diagnostics with the PRIMA Control System.

The Light source, the Phase meter and the Control Hardware sub-systems are all located inside the VLTI storage room (IC104).
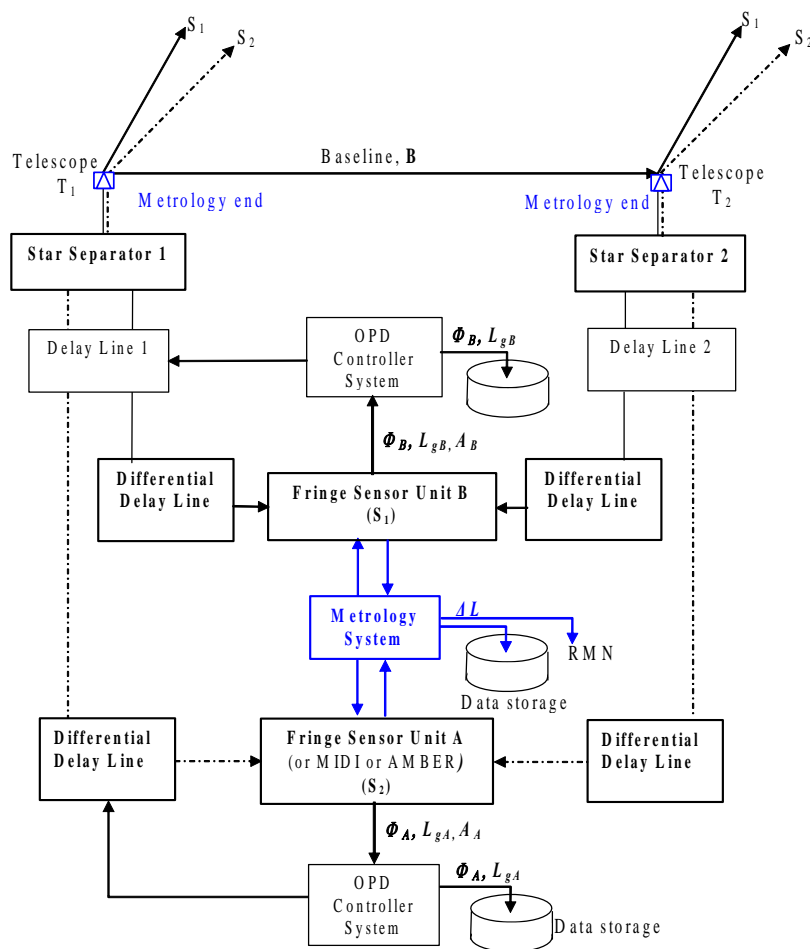

Figure 1   Functional block diagram of PRIMA and its sub-systems.
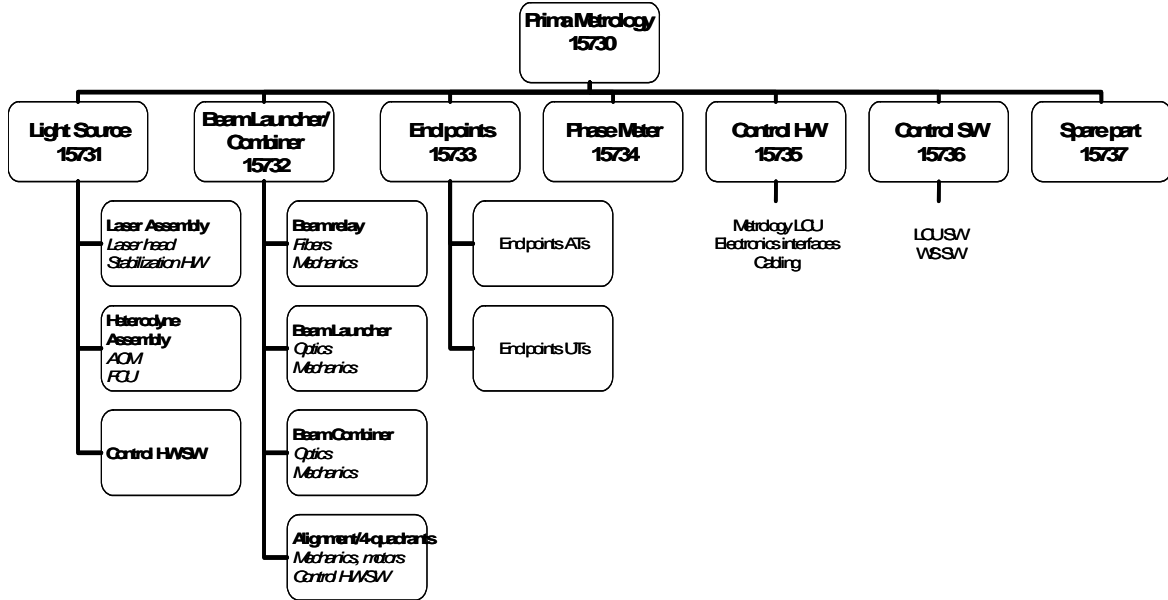
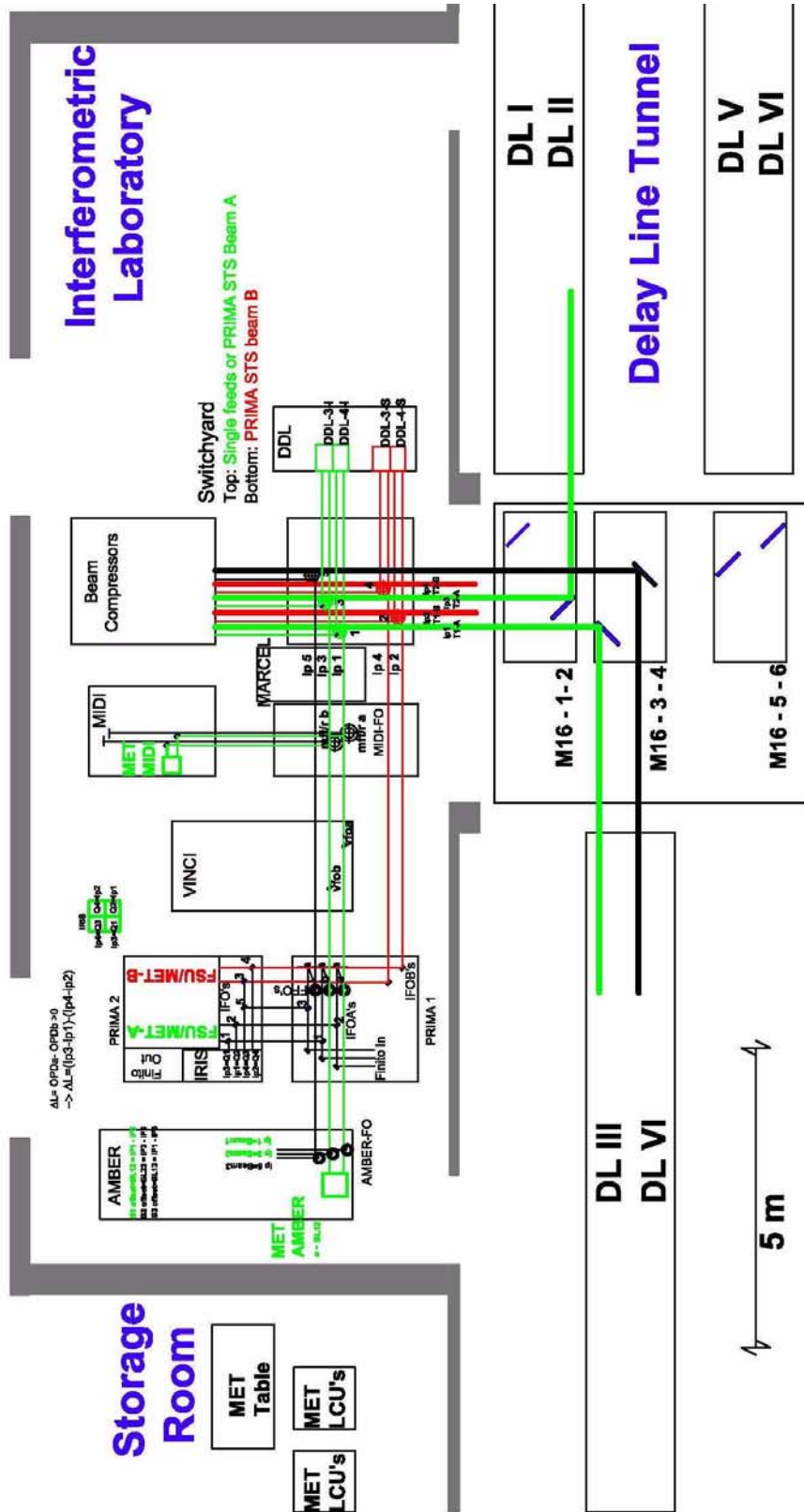*Figure 2   Sub-system breakdown*

Figure 3   *Overview of the location of the metrology hardware: 1 optical table and 2 electronic cabinets are located inside the storage room. Four beam launcher/combiner areas inside the interferometric laboratory located on the Amber, FSU#A, FSU#B and MIDI tables.*

An overview of the metrology hardware is shown in Fig. 5. The light of a frequency stabilized Nd-Yag laser (*Laser Assembly*) is split into four frequency shifted laser beams by an *Heterodyne Assembly* (see section 7). The pair of beams attributed to Channel B is relayed towards the *Beam Launcher/Combiner* of the FSU#B through optical fibers (*Beam Relay*). Similarly, the pair of beams attributed to Channel A is relayed towards the beam launcher/combiner of FSU#A, or MIDI or AMBER, as described in Table 1.

This fiber "multiplexing" will be performed manually from the VLTI storage room, according to Table 1. In order to simplify Fig. 5, only two beam launcher/combiners are shown. The status of the fiber connection is read by inductive sensors.

The metrology beam launcher/combiner for AMBER and MIDI are independent of the MIDI and AMBER optics. For both FSU'sthe superposition of the laser beams after a round trip in the VLTI is done by the FSU beam combiner.

All conventions used by the metrology system are described in RD 16.

Table 1   Configuration of the metrology Channels as a function of the PRIMA observing modes

Metrology Channels	PRIMA Astrometric Mode	PRIMA Imaging Mode
Channel A $\nu_{laser}+38MHz$ $\nu_{laser}+38.65MHz$ Beat signal=650 kHz	FSU #A	MIDI or AMBER
Channel B $\nu_{laser}-40MHz$ $\nu_{laser}-39.55MHz$ Beat signal=450 kHz	FSU#B	FSU#B

In each metrology channel, the metrology beams are first superimposed to create a _reference_ signal which monitors the OPL variations from the laser to the beam launcher/combiner (i.e including the fibers). Then the beams are launched separately in the stellar paths. After a round trip through the VLTI, the beams are recombined to form a _probe_ signal. Both *reference* and *probe* signals are relayed through optical fibers towards the *Phase Meter (see section* 10)*,* where they are detected and processed to generate the quantity $\Delta\phi=4\pi/\lambda.\Delta L$, as sketched in Fig. 4.

The information about the OPD of channel A is carried in the phase of a 650 Khz beat signal. Similarly the information about the OPD of Channel B is carried in the phase of a 450kHz beat signal. The phase meter internally mix these 2 beat signals such that ΔL is measured using the phase of a 650kHz-450kHz=200kHz beat signal. The reasons why the phase meter generates directly the quantity ΔL (internal electronics) is to reduce the measurement noise. The phase variations of ΔL are slower compared to individual OPD's.

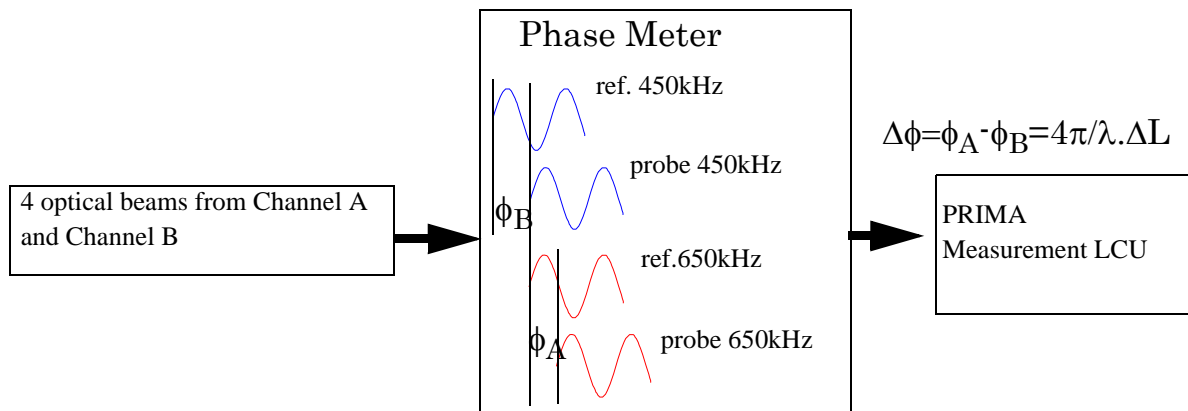Details about the phase meter are described in RD 11

Figure 4   Functional sketch of the Phase detection

The metrology control electronics is integrated inside two electronic cabinets located inside the VLTI storage room. The two metrology cabinet host:

- 1 *Phase meter crate*: This crate detects the metrology beams and process them to compute the differential optical phase variations: $4\pi/\lambda.\Delta L.$, with $\Delta L = OPD_{CHA} - OPD_{CHB}$. It also delivers a set of diagnostic data.

- 1 *"acquisition" LCU crate (lprmac)*: this LCU computes at up to 8kHz the quantity ΔL based on the phase and status data delivered by the phase meter and writes the results on the reflective memory network

- A clone of the above phase meter and its acquisition LCU (lprma2). This clone has been introduced to enable the calibration of FSU#A and FSU#B by deriving the quantities OPD_{CHA} and OPD_{CHB} from the following measurements:
  $\Delta L(lprmac) = OPD_{CHA} - OPD_{CHB}$ and $\Delta L(lprma2) = -OPD_{CHB}$
  Both measurements are written on the RMN.

- 1 *"Pupil tracker" LCU crate (lprmpd)*: this LCU reads the 4-quadrant detectors and send the appropriate corrections to the STS to maintain beam alignment.

- The electronics of the *Light Source* consisting of the *Heterodyne assembly* and of the electronics of the *Laser Assembly.*

- 1 "light source stabilization" LCU (lprmls) which runs the control loop of the frequency stabilization of the laser, and read the laser diagnostics and the status of the fiber connections

The individual OPDs derived from $\Delta L(lprmac)$ and $\Delta L(lprma2)$ could be used by the OPD controller to reduce internal vibrations. There 2 limitations:

- the OPD are monitored up to the STS (i.e it does not include the coude train)

- the error on the measured OPD due to residual fluctuation of the laser frequency will potentially reach about 0.6 nm rms per m of OPD[1]. For an OPD of 120m, the error becomes 72 nm. The measurement range is 346 mm. After this value, the phase meter overflows and the data are wrapped.

All the hardware located inside the storage room (control electronic, light source, beam relay) is common to all metrology configurations. The differences only concern the beam launcher/combiners, that is the way the metrology beams are physically injected and extracted in/from the various stellar paths.

Finally an laser interlock system based on Siemens safety PLC is implemented to guaranty the safe operation of PRIMET as described in RD 4 and RD 14.

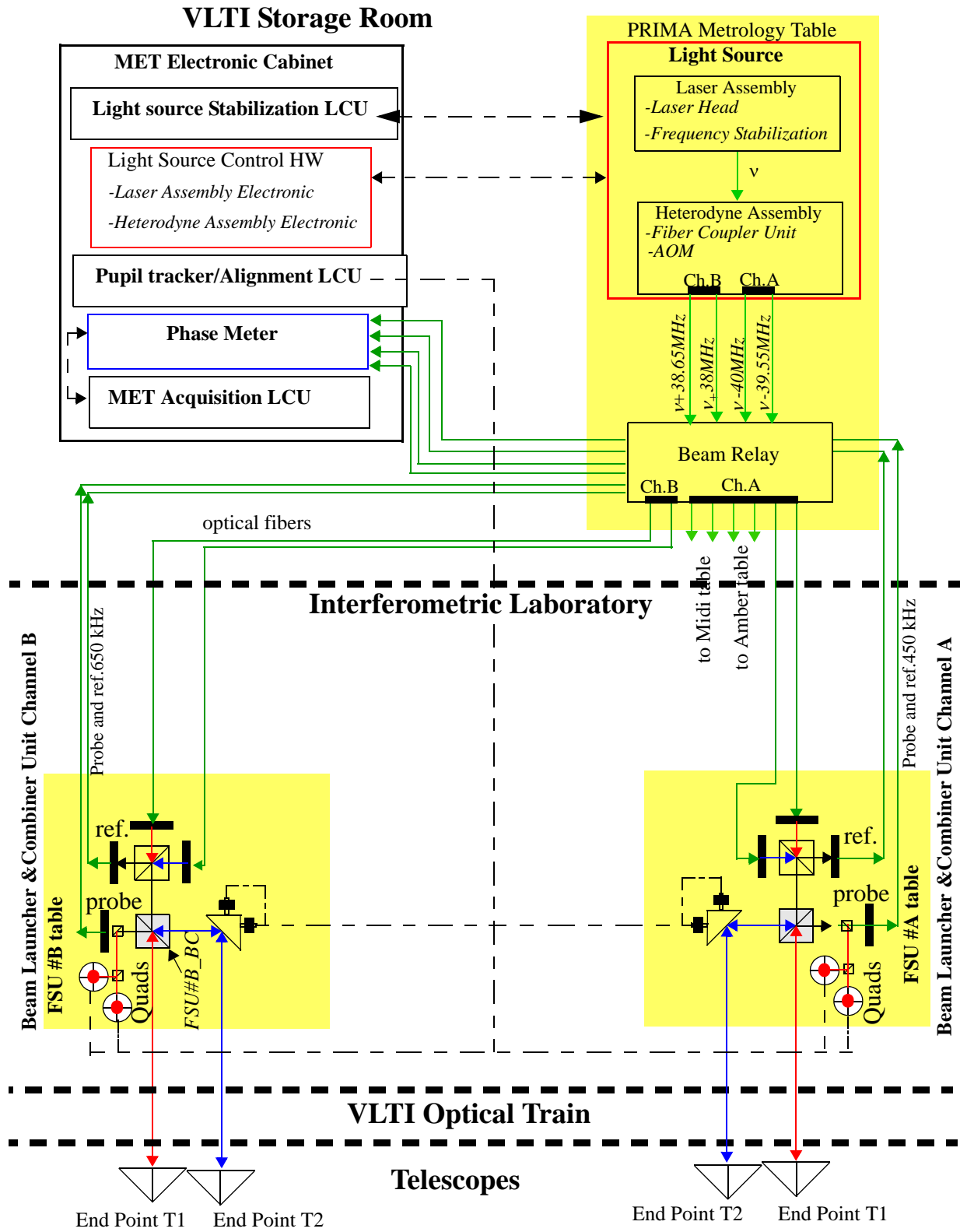
1. based on a 150 kHz rms residual frequency fluctuation.

Figure 5   *PRIMA Metrology hardware Overview: green lines represents optical fibers; dashed lines represents control lines. ν=c/λ represents the frequency of the laser*

6 Design and implementation for the FSU Channels

6.1 General configuration

For each FSU channel, a pair of frequency shifted laser beams are relayed from the storage room through two SM-PM input fibers. These beams, which are linearly polarized but with orthogonal directions (s and p), are first super-imposed on a polarizing beam splitter. On one side of the beam splitter, a reference signal is created to monitor the overall optical path variations that occurred along the input fibers.

On the other side of the beam splitter, both super-imposed laser beams further propagate towards the FSU dichroics and the central part of the FSU-BC. This area corresponds to an image of the VLTI central obstruction (considering that a pupil image is formed on the FSU_BC). The metrology beams will only use a 2.5 mm diameter disk centered on the FSU_BC.

The central part of the FSU_BC is used to separate both s and p polarizations in each VLTI arm and recombine them after a round trip through the VLTI. In this way, the monitoring of ΔL starts from the Beam Combiner of the FSU such as to minimize the measurement error. The central part of the FSU_BC consists of a non-polarizing Beam Splitter with integrated Linear polarizors.

The FSU-BC include two wedged surfaces such that any metrology light back-reflected from the surface of the FSU-BC is not coupled into the FSU input fibers (refer to section 6.5 for details).

The principle of the Metrology beam separation and recombination of the FSU channels in shown in Fig. 6. The optical configuration of the metrology beams for each FSU Channel in shown in Fig. 7.

It is important to minimize the polarization leakage after the FSU_BC. This means that only one frequency shifted beam should propagate in each arm of the interferometer. Otherwise a cyclic measurement error will occur with a period corresponding to an OPD fluctuation of $\lambda/2$. The amplitude of this error depends on the amount of leakage. The source of errors leading to polarization leakage are shown in Fig. 8, as well as the associated alignment requirements needed to minimize the polarization leakage error.
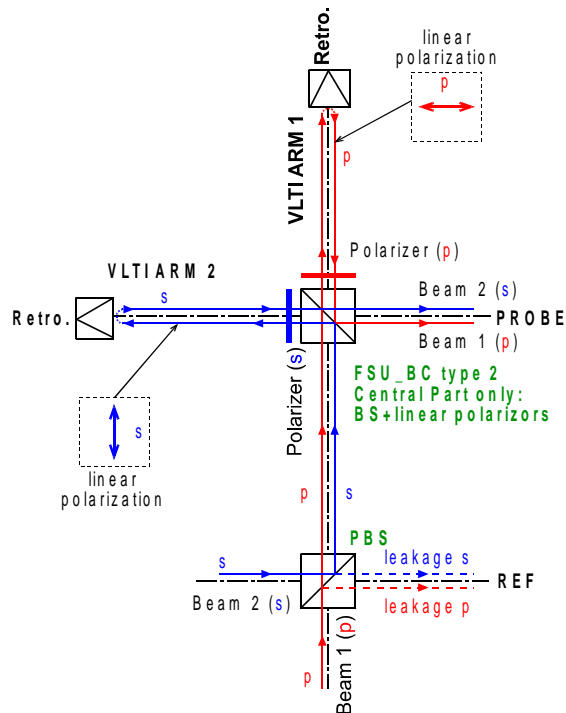
Figure 6   *Principle of the Metrology beam separation and recombination of the FSU channels. The p and s beams are spatially superimposed. They are artifically separated on the above drawing to better illustrate the measurement principle.*
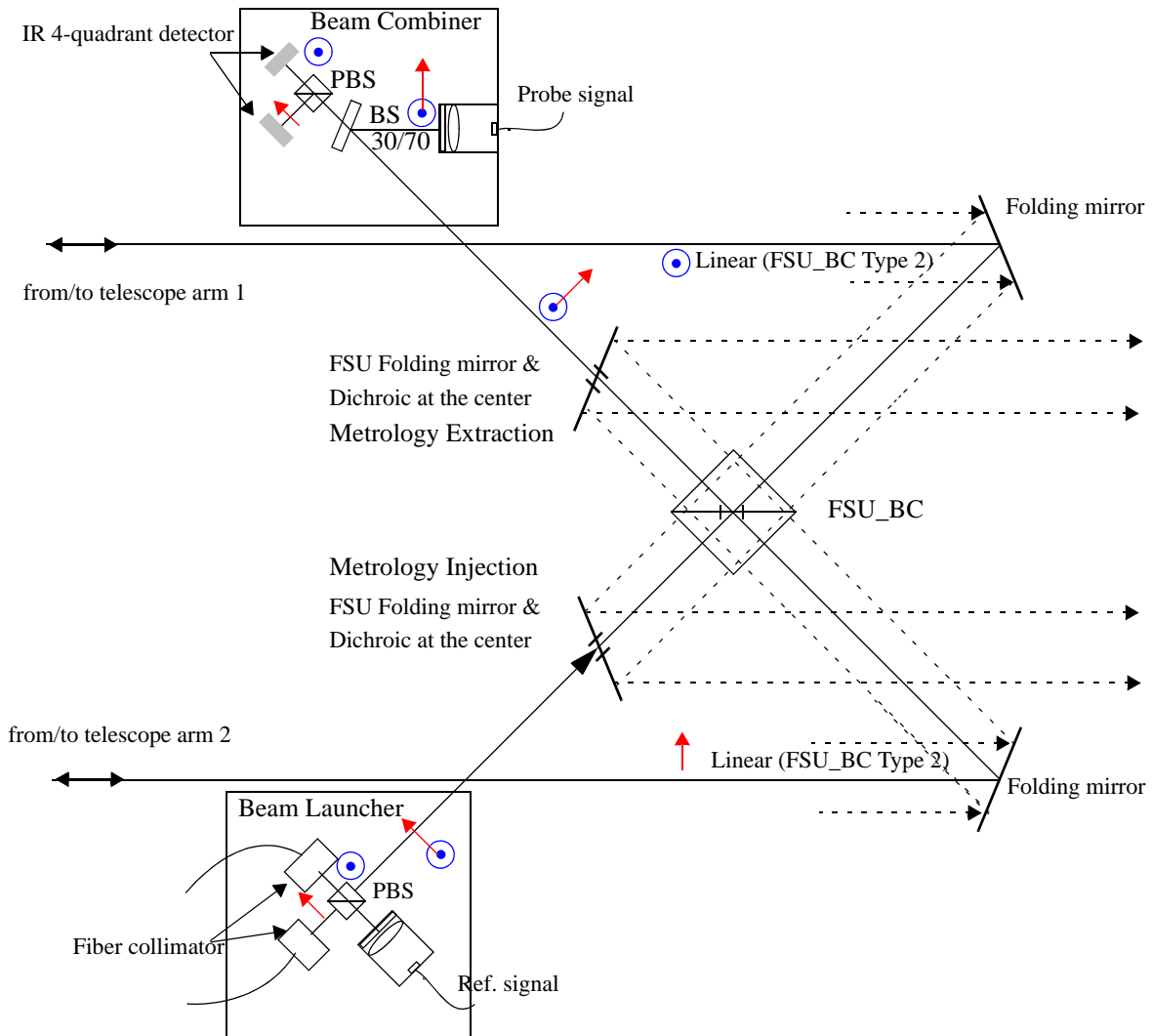
Figure 7   *Optical Configuration of the metrology beams for each FSU Channel.The solid lines represent the path followed by the metrology beams. The dotted lines represent the path of the stellar beams in the FSU beam combiner.*

Boundary limits for the definition of the metrology beam diameter:

Background:

The size of the waist of a Gaussian beam, W_0, is defined such that at a distance W_0 from the optical axis, the intensity is I_0/e where I_0 is the intensity at the center of the waist. I_0 is the peak intensity, not the integrated intensity over the beam surface. After a propagation path, z, the waist radius is $W(z)=z. \lambda/(\pi.W_0)$ (for $z>>z0=\pi.W_0^2/\lambda$). The divergence (full) angle is defined as $\theta =2.\lambda/(\pi.W_0)$.

In the VLTI laboratory, the diameter of the central obstruction of the 18mm diameter beam is:

- ϕM2(1116)/ϕM1(8000) x 18mm= 2.5 mm for the UT's

- ϕM2(138)/ϕM1(1820) x 18mm=1.36 mm for the AT's

For the FSU-BC, the central diameter reserved for the metrology is 2.5mm. During observation with the ATs, the mismatch between 2.5mm and 1.36 mm will introduce a power loss of only 1.4% for the stellar beam.

Selection Criteria

The metrology beam waist should be sufficiently large so that the divergence angle remains less than the unvignetted field of view of the VLTI optics. However, it must remain sufficiently small to maximize the energy inside the central obstruction. This will help: i/ to minimize the straylight seen by an instrument using a pupil stop ii/ to reduce the beam truncation (power loss & diffraction) due to the finite size of a retro-reflector located on M2 (TBD future upgrade).

Table 16   Summary of the possible the waist diameter

Criteria	UT
Fit inside central obstruction	$2.w_0 < 2.5$ mm
Divergence angle < VLTI F.O.V	0.4 mm $< 2.w_0$
Transmission through central obstruction > 99.9% > 99.5% > 99.0%	$2.w_0 < 1.3$ mm $2.w_0 < 1.52$ mm $2.w_0 < 1.6$ mm
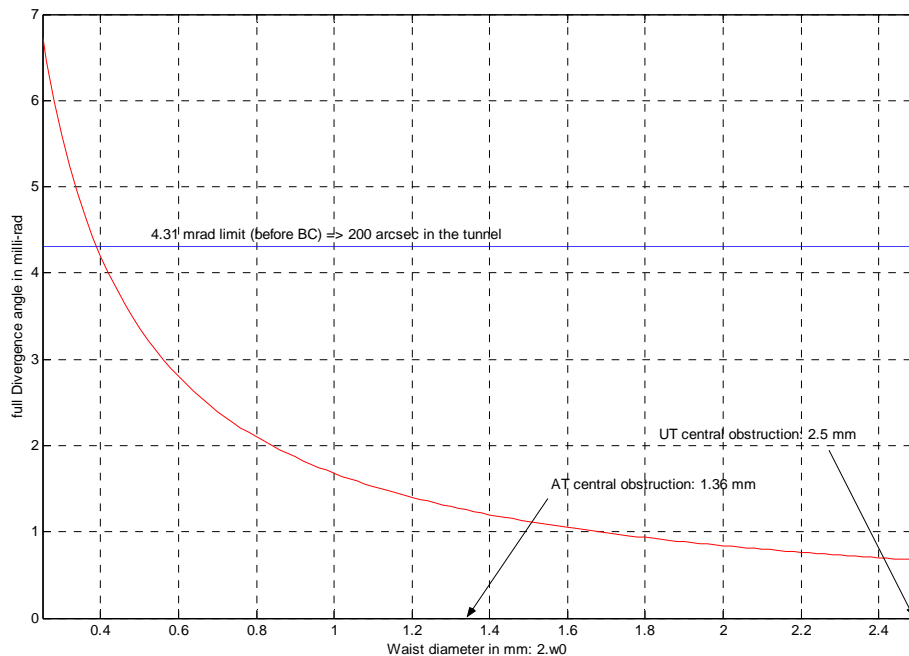
Figure 8

The final selection of the metrology beam diameter depends on several parameters:

*   *The motion of the metrology beam on the FSU-BC after a round trip through the VLTI due to misalignment or internal turbulence. The ratio between the metrology beam diameter and its <u>lateral displacement</u> or its <u>tilt</u> will define the visibility of the metrology fringes*

- *The <u>power budget</u> and the level of <u>straylight</u> authorized on the FSU detector.*

These aspects are detailed in the next sections.

6.2   Power Budget

A power budget has been derived for the FSU Channel based on the criteria that a minimum of 100nW must reach the metrology detector in any PRIMA configuration.

This value is based on the results obtained with the phase meter prototype. Indeed we know that an accuracy of 0.8nm (i.e at the 1 nm level) can be reached with an optical power reaching the detector of 20nW, for a fringe visibility of 70% and a 50 kHz bandwith. So the figure of 100nW is based on 20nW with a safety factor of 5.

The transmission of the VLTI at λ=1319nm has been measured during a metrology test campaign. The worse configuration in terms of transmission corresponds to an observation in the STS calibration mode with the FSU-BC. In this condition, the laser power at the output of the heterodyne assembly must be larger than **15mW** at λ=1319nm.

6.3   Impact of the laser beam tilt and lateral displacement

6.3.1   Tilt error on the FSU_BC

The metrology system operates in a "retro-reflection" configuration and consequently, by first order approximation, it should not be affected by tilt errors. However, measurements performed at Paranal have shown that we can expect a 0-to-Peak tilt error of 44.4 arcsec in the laboratory (i.e 100marcsec_sky for the UT's and 444marcsec_sky for the ATs).

Depending on the metrology beam diameter, the consequences on the visibility loss and on the injection of the metrology beam into the probe fiber were analyzed in a Tilt budget. The results are summarized in Table 2 for three beam diameters. For a tilt error of 44.4arcsec in the lab., the conclusions are:

- The visibility loss will remain <2% for any beam diameter smaller than the central part of the FSU_BC reserved for the metrology beam

- the angular size of the probe fiber will always be sufficiently larger than the tilt error so that an optimum coupling can be maintained (no glitch, no significant power loss).

Therefore the tilt error has little impact on the metrology performance for the FSU channels. This conclusion assumes that the image of the VLTI pupils are correctly re-imaged on the FSU_BC.

Table 2   Summary of the impact of a tilt error of 44.4 arcsec_lab on the metrology beam

	Metrology Beam diameter		
	2.5 mm	2mm	1mm
Angular Size of the probe fiber[1] Single mode (core 9 μm, NA=0.11) Multimode (core 62.5 μm, NA=0.275)	1.72 arcsec_sky 28.3 arcsec_sky	2.15 arcsec_sky 35.4 arcsec_sky	4.3 arcsec_sky 70.7 arcsec_sky
Contrast loss for a tilt error of 44.4 arcsec_lab	2%	1.3%	0.3%
Lateral shift on the FSU dichroics[2] for a tilt error of 44.4 arcsec_lab	10μm	10μm	10μm

1. this size is calculated such that the beam focussed on the probe fiber fits the fiber NA
2. the dichroics are located 48 cm from the FSU_BC

6.3.2 Lateral beam displacement on the FSU_BC

The lateral beam displacement of the returned metrology beams must be minimized to ensure that:

- no glitch appears during the calibration and observation phase (otherwise the calibration must be performed again)
- there is sufficient fringe contrast (i.e the beams must sufficiently overlap)
- the straylight generated towards the FSU remains acceptable

An estimation of the maximum lateral displacement is given in RD 9:.**±1686** μ**m_lab** (Peak value, uncorrelated for 1 beam). The lateral displacement of the metrology beam must be stabilized to possibly operate in the central obstruction as designed in RD 9 (see also section 6.4).

For disturbances that are common to the metrology beams and to the stellar beams, a correction of the metrology beam position by the Star Separator VCM will also correct the position of the stellar beams (see Figure 10).

Section 6.4 describes the sensor and actuators selected for the correction of the lateral beam displacement.

Table 3   Summary of the impact of the lateral beam displacement on the contrast loss and power leakage

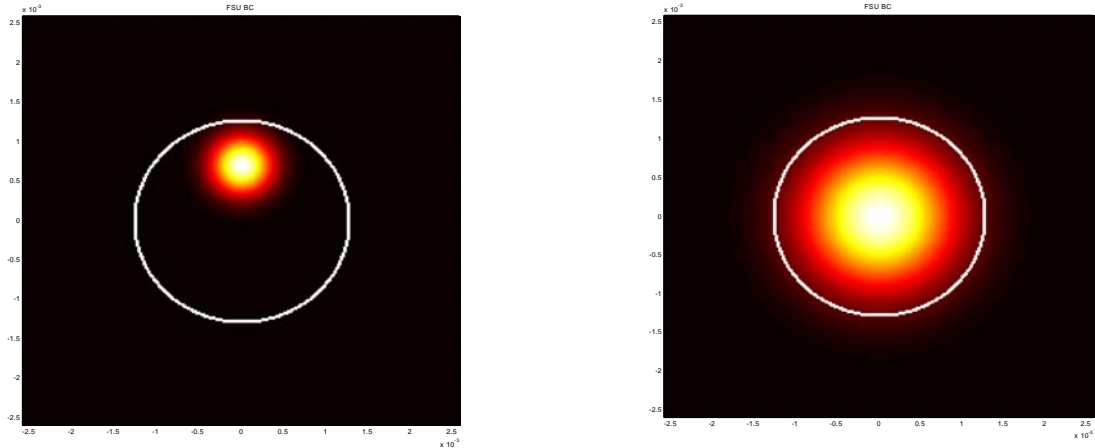| **Lateral Shift**	**Metrology Beam diameter**	**2.5 mm**	**2mm**	**1mm**
Residual Lateral shift of 100 μm (correction, Fcut=1Hz) *Contrast loss* *Power leakage*		10.2% 13.8%	12.7% 4.6%	25.3% 8.2e-4%

Figure 9   *Metrology beam at the center of the FSU BC. The white circle identifies the central area of the FSU-BC (2.5 mm diameter). This simulation was used to generate a metrology beam with a gaussian intensity profile and compute the portion of the metrology power leaking outside the central area for a given lateral shift. Left: beam diameter=1mm with a 700 μm lateral shift;Right: beam diameter=2.5 mm without shift.*
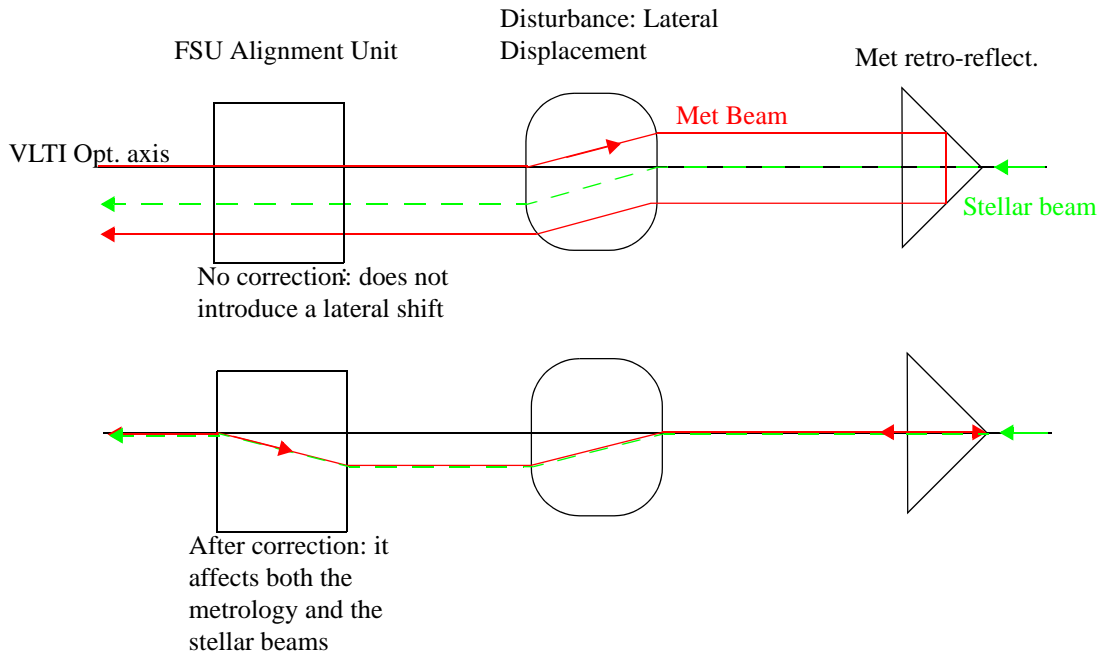

Figure 10   *This sketch shows that if the FSU Alignment unit corrects the lateral position error of the metrology beams introduced inside the VLTI, it will also correct the lateral position error of the stellar beam introduced by the same disturbance. The same conclusion applied to the correction performed by the Star Separator.*

6.3.3   Conclusion and selection of the beam diameter

The analyses presented throughout section 6.3 have shown that the tilt error of the metrology beam has little impact on the metrology performance for the FSU channels. However, the lateral position of the metrology beams must be stabilized at the center of the FSU-BC. Considering a correction bandwidth of about 3 Hz, the expected residual lateral displacement of the metrology beam should remain below 100μm (0-Peak), as shown in RD 10.

In this condition, the optimum metrology beam diameter is 1 mm (see Table 4). It allows minimizing the portion of the metrology power leaking outside the central obstruction (8.2 e-4%), while maintaining the contrast of the metrology fringes larger than 70% (design goal).

Table 4   Comparison of the performance obtained for 3 beam diameters, for a residual Lateral shift of 100 μm and a tilt error of 44.4 arcsec_lab

	Metrology Beam diameter		
	2.5 mm	**2 mm**	**1 mm**
Contribution to the Contrast loss			
Tilt (44.4 arcsec_lab)	2%	1.3%	0.3%
lateral displacement (100μm)	10.2%	12.7%	25.3%
Total	**12.2%**	**14%**	**25.6%**
Power leakage outside the central obstruction	13.8%	4.6%	8.2e-4%

In calibration mode, the metrology beam will be focussed on the slit of the M10 of the STS. This slit is 10 μm wide. The STS is F#36 for an input beam of D=80mm. Using a d=1mm metrology beam in the laboratory and a compression factor of K=4.44, the metrology spot will be on M10: $s=2.44.\lambda/d/K*(D*F\#36)$, i.e $s=2mm$. This should be sufficiently large to avoid significant power loss or diffraction effects.

6.4   Pupil tracking

A full description of the pupil tracker can be found in RD 8 and RD 9.

The measurement and correction of the lateral beam displacement will be performed for each metrology beam by a pupil tracker. The lateral beam displacement is measured by an IR 4-quadrant detector, and corrections are computed by an LCU (lprpmd) and sent to the corresponding STS-VCM.

As shown in Fig. 7, the "s" and "p" retro-reflected metrology beams are superimposed at the level of the FSU-BC. Then 70% of the flux is reflected by a BS to generate the Probe metrology signal, whereas 30% will further propagate towards a PBS. This PBS separates again the "s" and "p" components on two different 4-quadrant detectors.

6.4.1   4-quadrant detectors

The 4-quadrants detector is a custom made low noise IR detector based on a IGA 030QD from ELECTRO-OPTICAL SYSTEMS INC (EOS).

It consists of:

- 1x detector head: 1 InGaAs 4-quadrant chip, low noise transimpedance amplifiers (BP~1.5 kHz), followed by a pro-grammable gain (PGA). The gain of both amplifier can is SW selectable.
- 1x30m cable relaying the signals Q1, Q2, Q3, Q4 to the acquisition module located in the metrology Cabinet (storage room).

- 1 acquisition module (1 module 3HE-8TE per 4-quadrant detector). This module filters the quadrant signals and provides power to the detector head. The filters are 5th order Butterworth filters (MBF), with a bandwidth of 274 Hz.

- 1x 19 inches rack which hosts up to 8 acquisition modules and 1 power supply

Each acquisition module provides 4 analog signals (Q1, Q2, Q3, Q4) which are read by a 16 bits Analog input board (VMIVME3123) located inside the Position sensor LCU of PRIMET. The Voltage range of each Q is [0-10V]. The LCU computes the lateral beam displacement of each beam using TAC.
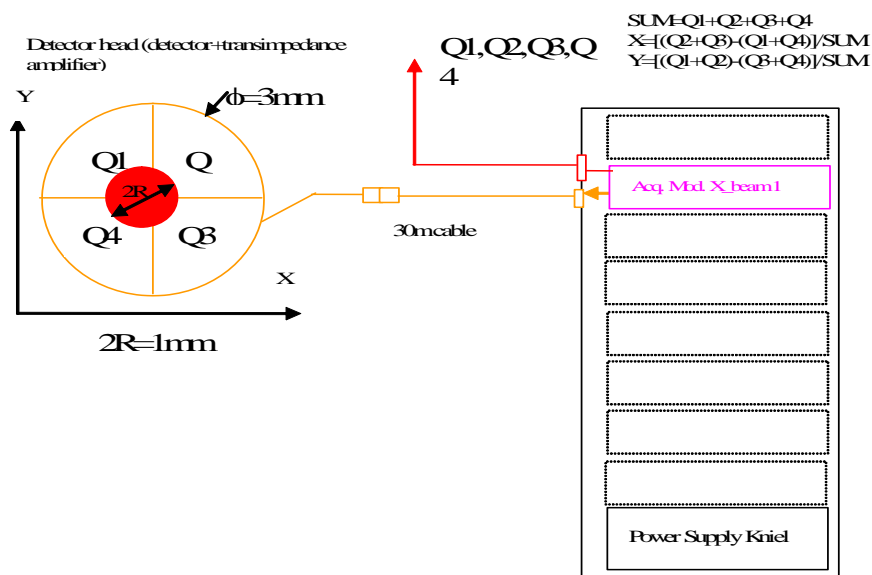

Figure 11   4-quadrant detector system

Performance of the detector:

- Analog Bandwidth: 274 Hz

- Voltage range of each Q: [0-10V]

- Sensitivity: 13nW/V (for a the gain no 3 of the transimpedance (Rf=10MOhm) and a gain of the PGA of 10, i.e a total gain of ~100)

- ADC: 16 bits over [0-10V] (VMEVMI-3123)

- Sampling frequency: Selectable (given by the LCU reading frequency)

- Measurement range: Given by the beam radius: baseline R=500 microns

- Voltage noise (Dark noise with Transimpedance=1e6 & PGA gain=100): 3mV (rms) and 20 mV (PV)

- Measured displacement noise for mean SUM=4V (i.e 52nW on overall detector using sensitivity 13nW/V)

    0.457% (PV) of a 1 mm radius= 4.57 microns (PV)

    775 ppm (rms) of a 1 mm radius= 0.78 microns (rms) (includes mechanical instabilities of set-up+ overall acquisition chain, Transimpedance=1MOhm; PGA=100)(see details in dedicated test reports)
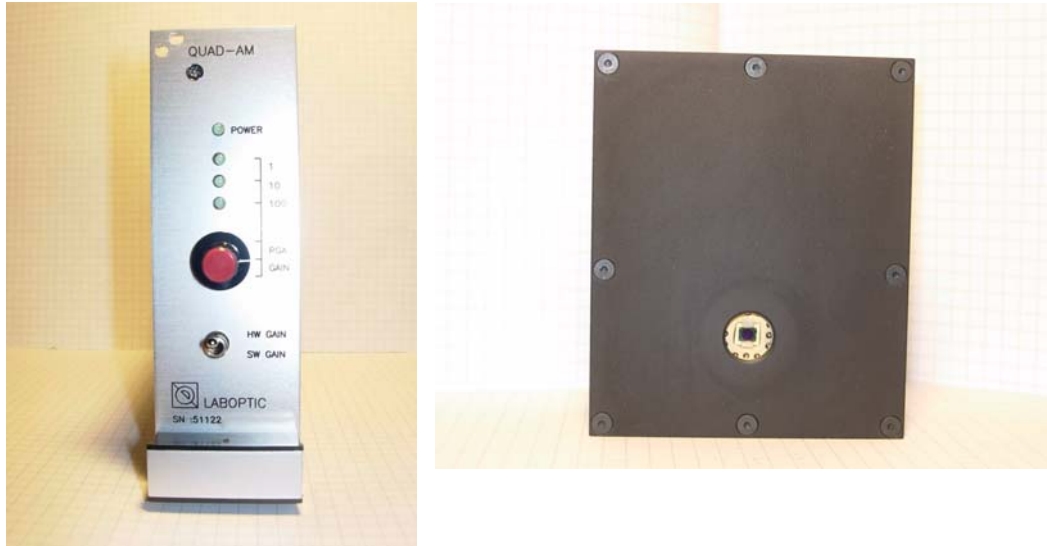
Figure 12   4-quadrant detector and its associated Acquisition Analog module

6.4.2   Actuators

The lateral position of a given metrology beam is controlled by tilting the corresponding mirror M14 (VCM) of the STS, located in an image plane. Each STS includes two M14 to control the lateral position of Beam A and of Beam B of the STS. The M14 are controlled by sending offsets in then [U,V,W] coordinate system of the light duct to the STS VCM LCU. The commands are interpreted by the STS LCU and forwarded to the piezo controllers of the mirrors.

6.4.3   Control architecture

Four active detectors are simultaneously operated. They correspond to the metrology arms monitoring the input channels Ip1&Ip3 (channel A) and Ip2 and Ip4 (Channel B=metrology channel of FSU#B). All four detectors are read by the Pupil tracker LCU (lprmpd).

This LCU converts the quadrant voltages into beam lateral displacement in the sensor's coordinate systems and computes the necessary corrections in the [U, W] coordinates system of the light duct for the selected star separator.

The corrections are sent as offsets to the current position of the VCM (similarly to the offsets sent by IRIS to the telescope's X-Y table). The lateral beam displacement and the corrections are computed at a frequency fs, but the corrections are sent at a frequency fc.

The corrections are sent using a dedicated LAN between the Metrology Alignment LCU and the STS LCU.
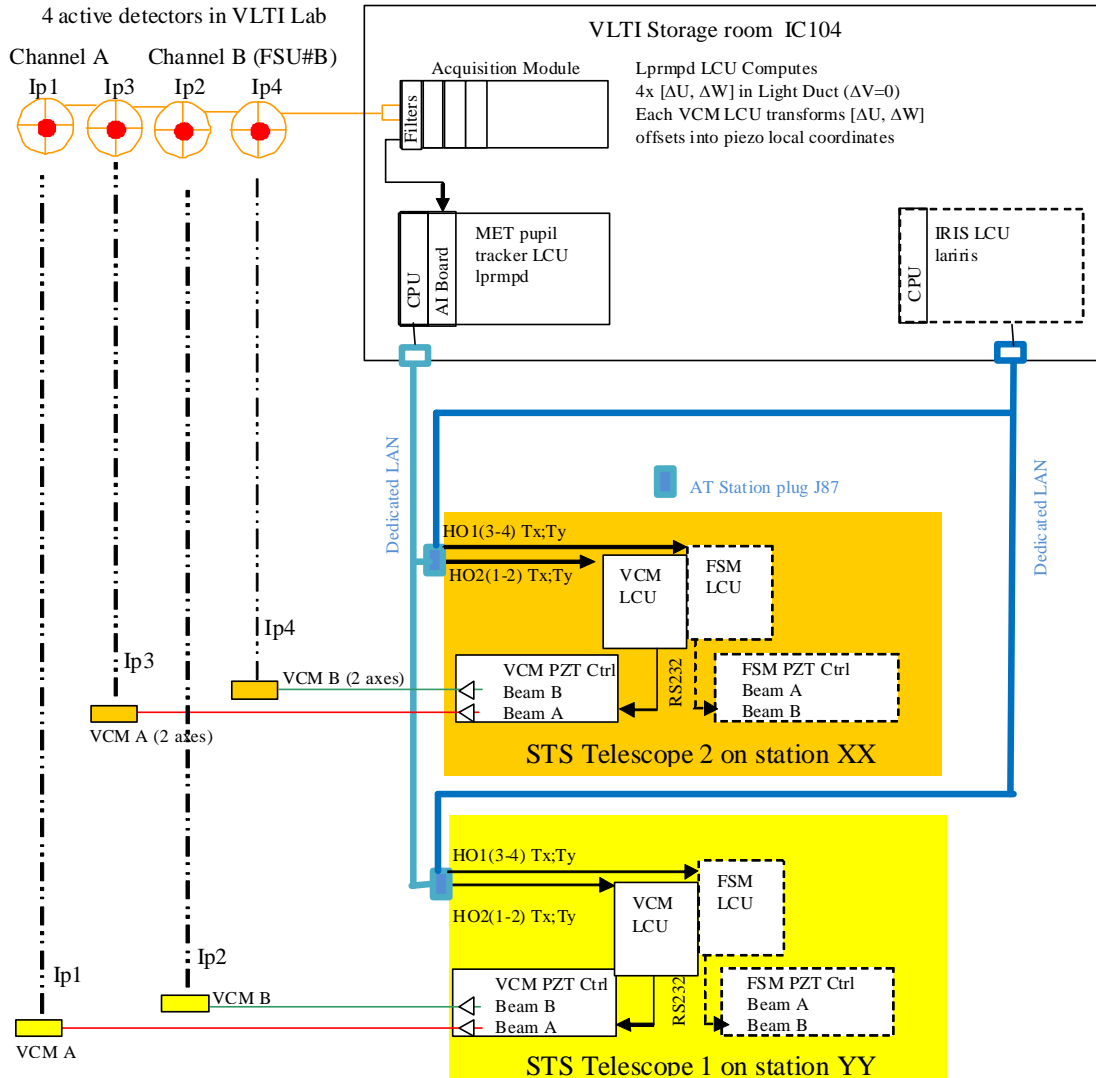
Figure 13   System architecture for the pupil tracking
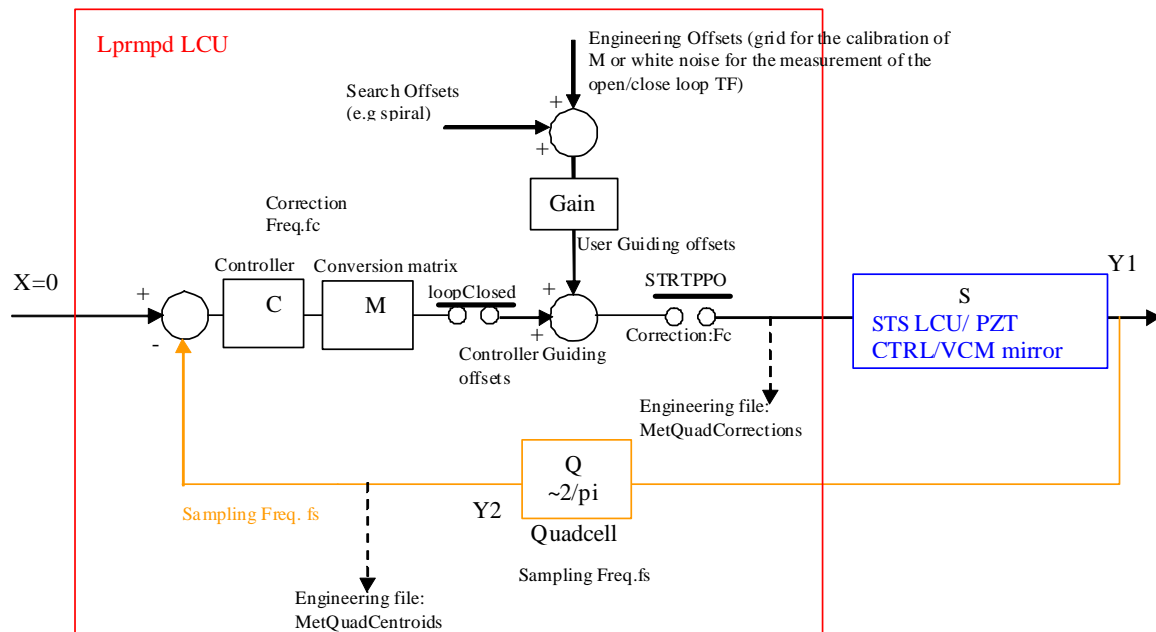
Figure 14   Control architecture for the pupil tracking

Control Hardware and control Software

A description of the pupil tracking control hardware can be found in RD 8 and RD 13.

A description of the software features and of their implementation can be found in RD 9 and RD 15

6.4.4   Performance

The performance of the pupil tracking loop as tested on STS AT#1 in Garching is documented in RD 10. It also includes a detailed description of the control loop.

After characterizing the various loop delays and limitations, a baseline controller has been defined. Its ability to filter pupil motion has been analyzed using open loop pupil motion data recorded on 29/10/06 at Paranal (50 files of 1 min distributed along the night),

The conclusion is that expected residual beam radial motion reaches a maximum of 2.5% rms of the metrology beam diameter. This value was reached once and was dominated by residual vibrations located in the 10Hz region. These vibrations are attributed to a bad tuning of the AT axis and should not be representative of the future operating conditions (pupil motion dominated by turbulence). A part from this case the residual beam motion is limited to 1% rms, or 6% Pk (which is compatible with the specs of 10% of the beam diameter,RD 9).

Additional tests were conducted in May 2008 at Paranal on STS-AT#4. Preliminary results indicates that the specification are met while operating on a short light duct. Measurements were performed on the G2 maintenance station, with DL#2 at OPL=14 m. In addition the enclosure of AT#1 and AT#2 were opened to increase air circulation inside VLTI (external wind speed ~ 8 m/s).

The residuals were dominated by a 46 Hz eigen frequency whose origin has not been yet determined. The pure delay of the system was 20msec compared to 15 msec measured in Garching. The difference may come from the fact that the vcm was connected to its pressure chamber at Paranal using a rigid "tube", thus changing the dynamic response of the VCM. Investigations are in progress.
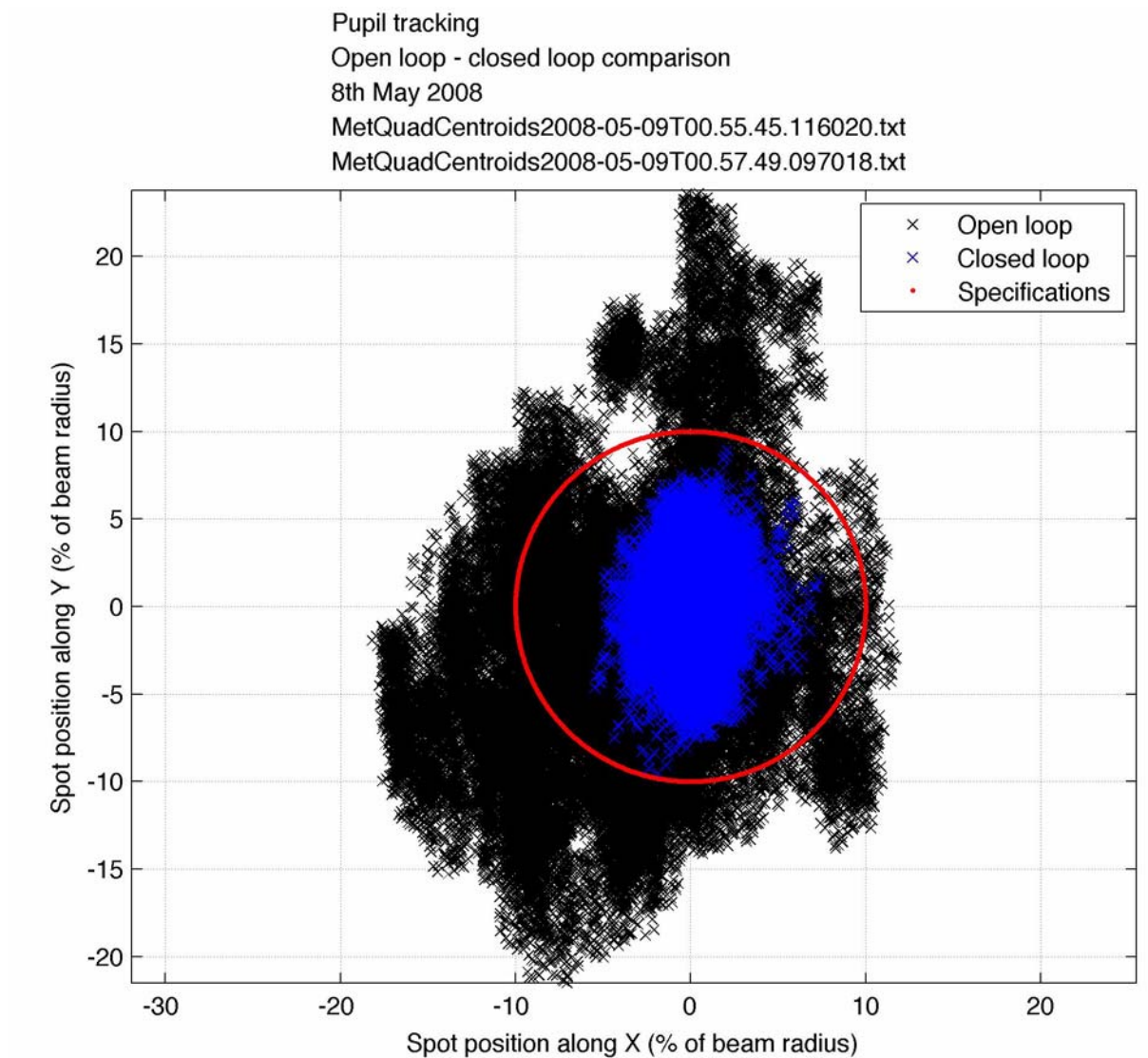

Figure 15   *Laser Beam centroid position measured by a 4 quadrant detector located on the PRIMA 2 table. Open-loop and closed-loop positions are recorded during 1min in each case with a sampling frequency of 1 kHz and a correction frequency of 100 Hz. The closed loop bandwidth of the system is 2.5 Hz.*

6.5 Straylight

As described in RD 5, the maximum straylight measured on one active pixel of the FSU corresponds to 600 ADU for a two second exposure and for an incident power of 0.6 mW per beam. For a 1 s exposure and for an incident flux of 0.5 mW per beam (as expected during operation), the straylight amounts to 0.3 ADU, i.e 2.7 electrons. This is 1000 time less than the thermal background (2700 electrons)

6.6 PRIMET Beam launcher & combiner in the FSU channels

The laser beams are launched in the FSU using 2 optical collimators and a beam splitter mounted on a 5-axis opto mechanical block from Newport (M-562F series). The superimposed laser beams can be:

- translated along X and Y and tilted around [X,Y,Z] using lockable AJS-127TPI-0.5 H screws.

- rotated along Z using a lockable goniometer (to minimize polarization cross-talk)

After a round trip through the VLTI, the metrology beams are spatially superimposed on the FSU_BC and are then extracted towards the PRIMET beam combiner bloc. At this location, the metrology "fringes" are generated using a 45 deg linear polarizor, located in front of the "Probe" fiber port. (see Fig. 7).

The beam launcher and beam combiner are equipped with fiber collimator and beam splitter bases from OFR, mounted on a common steel base plate. The fiber collimators include a collimated lens which can be translated to adjust the tilt and focus of the output laser beam. The fiber remains fixed with respect to the collimator housing. The lateral position of the fiber collimator is adjusted by design with a precision <100μm.

The **beam launcher** (i.e. beam injection) of each FSU channel is made of the following components:

Collimator lens: OFR-LLO-PAF-5-1319nm;

This lens will be used to collimate the frequency shifted beams of Channel A.

Aspherical lens f=5mm; AR coated. For a fiber mode diameter of 9μm, the diameter of the beam ($1/e^2$) on the lens will be 0.93 mm at λ=1319nm. The angular size of the fiber core is 370 arcsec_lab (6.2 arcmin) in the laboratory. This corresponds to 3.7 arcsec_sky for the AT's.

For the "ref." signal, a multimode fiber will be used with a core of 62.5 μm (NA=0.275), i.e 7 times larger than the single mode core. Its angular diameter will also be 7 times larger, i.e 2590 arcsec_lab. The diffraction spot on the ref fiber for a 1mm beam is 345 arcsec_lab, so the metrology spots will fully remain within the core of the reference fiber. The NA of the focussed beam is about 0.1, thus less than the NA of the fiber for optimum coupling.

Collimator port: OFR-PAF-X-SM;

5 axes fiberport with FC/PC bulkhead (2mm key for single mode for the input fibers or multimode fibers for the "ref." signal)

Lens translation range: >1 mm (for a lens of f=5mm, the adjustment range of the tilt of the collimated laser beam is >11 degrees)

Tilt sensitivity of the collimated laser beams is ~ 30 arcsec)

The key of the collimator ports of the input fibers will be oriented at 90degree such that the frequency shifted input beams are orthogonally polarized. The required angular precision is 1.5 arcmin. This can also be achieved by introducing half wave plate (or a linear polarizor) at the output of the fiber port

Polarization Beam Splitter: OFR-PSCL-B-1319nm

It is used to generate the reference signal.

Size: 4x4 mm; Tp/Ts>1000:1; Tp>97%; Rp<1.5%; Rs>98%; AR coating on 4 sides

Flexure stage supporting the Beam splitter: "Aiming base" OFR-ACB3 rotation available

θ_x, θ_y, θ_z

Half-waveplates: OFR-RZB-1319nm;

Aperture (custom): 5mm; AR coating. These plates are used to adjust the orientation of linear polarization of the beams at the output of the collimator port.

Sensitivity of the angular alignment: <1.5 arcmin

Linear Polarizor: OFR-PCB-5-1319;

aperture (custom) 5mm; WFE<λ/8; Tp>98%; Extinction ratio >20000:1. It is used in front of the "probe" collimator port for the generation of reference interference fringes.

Sensitivity of the angular alignment: <1.5 arcmin

Base plate: OFR 100mmx50mm custom steel plate

The base plate is fixed to a 5 axes alignment stage used to bring the superimposed metrology beams on the center of the FSU_BC and aligned along the VLTI optical axes

The PRIMET **beam combiner** of the PRIMET FSU channel is made of the following components;

Collimator lens: OFR-LLO-PAF-5-1319nm;

This lens will be used to focus the probe fringes on the probe fiber

Aspherical lens f=5mm; AR coated.

The "probe" fiber is the same multimode fiber as the 'ref' fiber, with a core of 62.5 µm and a NA of 0.275. Its angular diameter is 2580 arcsec_lab with f=5mm. The diffraction spot on the probe fiber for a 1mm beam is 345 arcsec_lab[2]. Even considering an image displacement of 44.4 arcsec_lab, the metrology spots will fully remain within the core of the probe fiber. The NA of the focussed beam is about 0.1, thus less than the NA of the fiber for optimum coupling.

Collimator port: OFR-PAF-X-MM

Same as for the Beam launcher, using a multimode fiber connector

Beam Splitter (BS) from "Laser component"

Size: 12.5 mm; AR coating on 4 sides; R=0.7; T=0.3. This beam splitter reflects 70% of the returned metrology beams towards the "probe" channel and transmit the rest towards a PBS.

Polarization Beam Splitter (PBS): from "Laser component"

Size: 12.5 mm; Tp/Ts>1000:1; Tp>97%; Rp<1.5%; Rs>98%; AR coating on 4 sides

This PBS is used to split the beam coming from the 2 arms of the VLTI on the IR 4-quadrant detector.

Flexure stage supporting the BS and the PBS: "Aiming base" OFR-ACB3 rotation available

θ_x, θ_y, θ_z

Linear Polarizor: same as for the beam launcher

Base plate: same as for the beam launcher but 50mmx120 mm

The base plate will be mounted on the same 5 axes alignment stage as for the beam launcher.

The implementation of the Beam Launcher and Combiner in the FSU channels is shown in Fig. 16. The optical axes of the metrology beams are located at 160mm above the FSU breadboards, like the stellar beams.

The image of the VLTI pupil will be located at the center of the FSU_BC. The expected tilt error of the metrology beam after a round trip through the VLTI is 44 arcsec_lab. This will introduce a contrast loss of about 0.3% on the "probe" fringes as shown in Table 2. However, considering that the distance between the FSU_BC and the 4-quadrant

---

2. $4\lambda/\pi/$waist

detector is about 350mm, the cross coupling between tilt and lateral displacement recorded on the detector will be 75µm. This remains below the criteria of 100µm used in Table 4.

The beam splitter used for the beam combiner (12.5mm) is large enough to cope with the expected "AC" fast lateral displacements (without corrections) of +/- 400 microns identified in Table 3
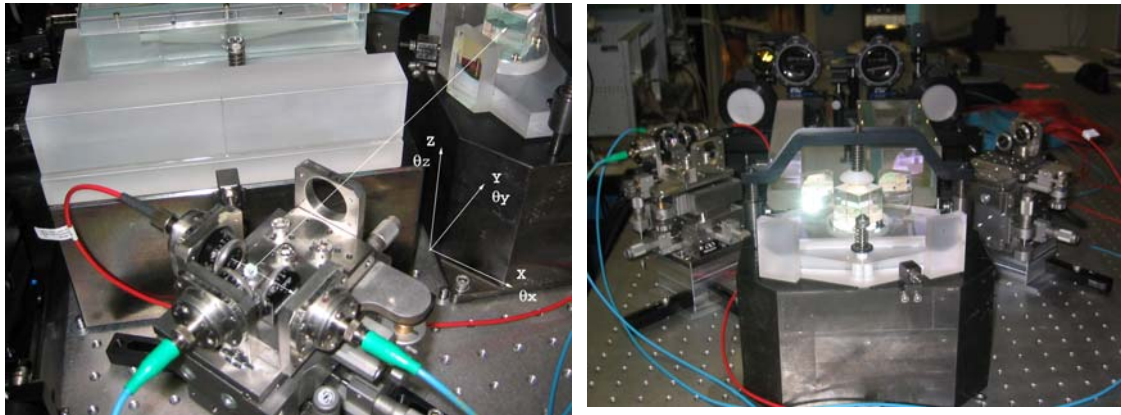

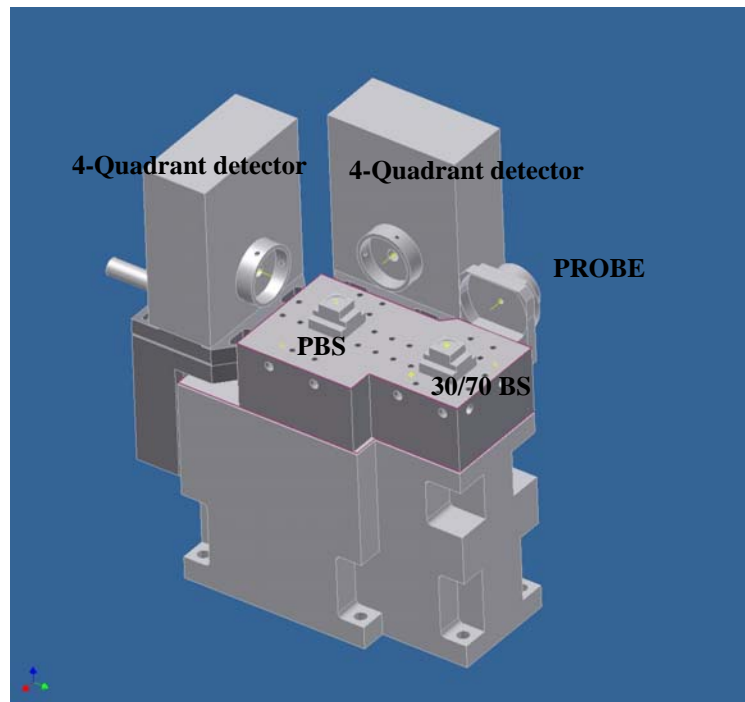*Figure 16   Beam injection (left) and extraction (right) in the FSU*

Figure 17   Support for the beam extraction, including the two 4-quadrant detectors

7 Light source

7.1 Introduction

The *Light Source* sub-system provides to the "PRIMA Metrology Beam Relay" four laser beams precisely defined in terms of wavelength, coherence length, frequency stability, optical power, and polarization state as specified in Table 5 and Fig. 19. The light source includes two sub-system: the Laser assembly and the Heterodyne assembly.

The Laser Assembly consists of a laser head associated with its frequency stabilization hardware. This stabilization hardware generates an error signal proportional to the laser frequency shift with respect to a frequency reference. This error signal is acquired and processed by the stabilization LCU (lprmls), which then sends a frequency correction command to the laser driver. Finally, the Laser Assembly feeds the "Heterodyne Assembly" with the frequency stabilized laser beam.

The laser head is an Nd-Yag Laser (λ=1319nm) Innolight MIR 500NE-FC (Serial 1537-M330g) whose maximum output power reaches ~280 mW at its fiber output. It is foreseen to use as a spare Nd-Yag Laser Model 125 from Lightwave electronics (max power~ 160mW).
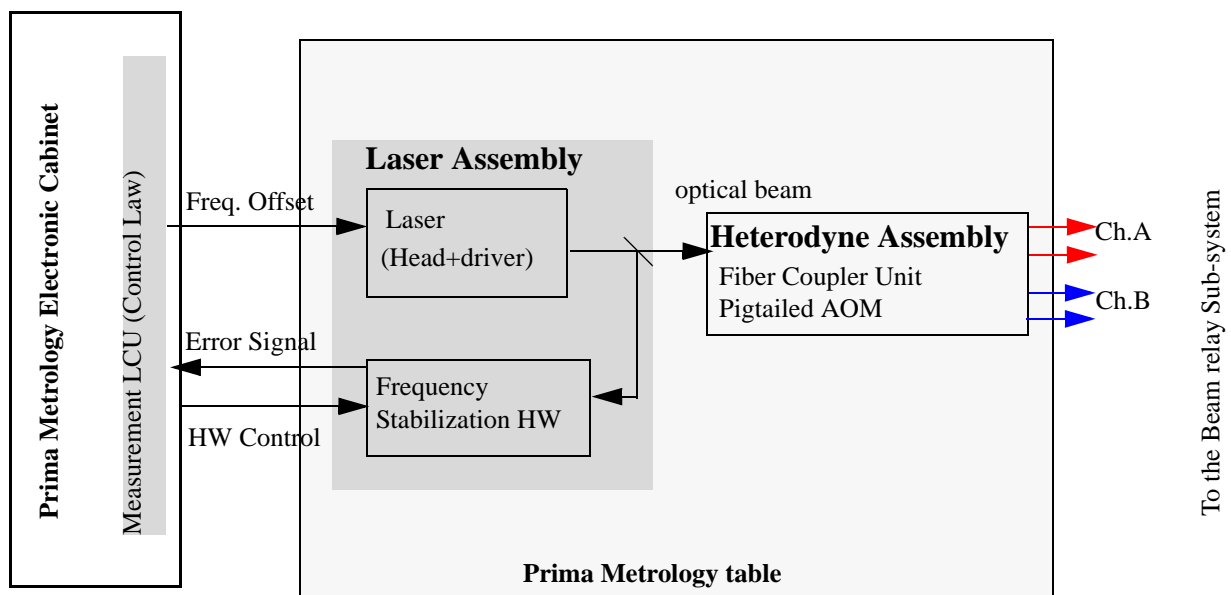

Figure 18   Block diagram of the Light Source System of the PRIMA Metrology, including the Laser and Heterodyne Assemblies

The specification for the laser beam delivered at each output of the heterodyne Assembly is given in Table 5. In particular the laser frequency stability must remain within $d\nu/\nu < 10^{-8}$ such that the associated metrology error remains below 0.6nm for a maximum value of ΔL of 60mm.

*Table 5   Specification for the laser beam delivered **at each output of the heterodyne Assembly***

Parameters	Specifications
Wavelength	λ=1319nm (ν=2.27.10^{14} Hz)
Optical Power	P>15 mW
Standard Deviation of the Power Intensity fluctuations	σ_P<0.1% rms (bandwidth 5Hz-10Mhz)
Linewidth/Coherence Length	$\delta\nu$< 5kHz over 1msec (L_c>>1000m)
Laser Frequency Stability	$d\nu/\nu$<10^{-8} or $d\nu$<2.27 MHz over the time window [125μsec to 1 hour]
Accuracy on the knowledge of the emitted frequency (includes periodic re-calibration)	$d\nu/\nu$<10^{-8} (lifetime)
Polarization state	Linear Extinction ratio: 20dB

The allocation of the frequency shifts is represented in Fig. 19. The associated heterodyne frequencies must be sufficiently high to possibly follow the OPL introduced in each channel (the fastest OPL variation being introduced by the Delay Lines).
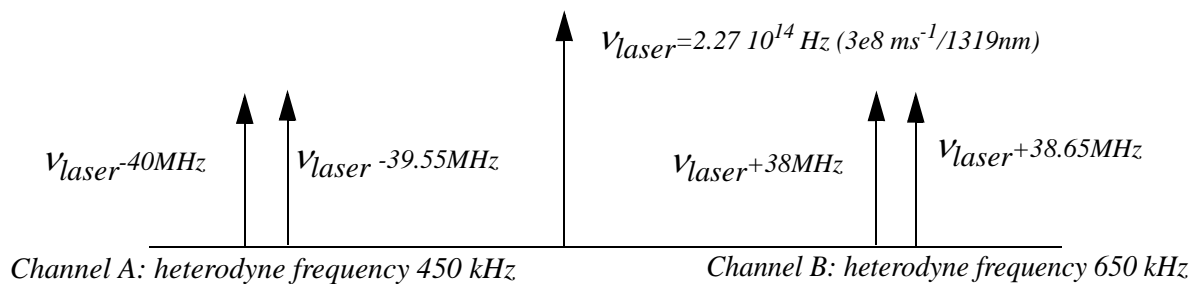

Figure 19   Heterodyne frequency allocation

7.2   Laser frequency stabilization

7.2.1   Design

The laser frequency stabilization is detailed in RD 6 and RD 7.

Algorithms and operations are described in RD 16 and RD 17.

the frequency stabilization is based on the Pound-Drever-Hall method where the absorption of molecular transition is used as a frequency reference. A part of the laser output power is frequency modulated and sent through a glass cell

containing Iodine (I2). If the laser optical frequency is within a transition the frequency modulation induces a modulation of the absorption, i.e an intensity modulation at the output of the cell, Figure 20. The amplitude of the modulation increases with the slope of the transmission spectra (with the distance from the center of the transition) and is zero at the center of the transition thus providing a good error signal. The rms amplitude of modulation is detected using a lock-in amplifier and is fed to a control loop.

In the case of PRIMET laser stabilization system, the laser frequency is corrected using two actuators:

- a fast actuator with a limited range of correction (+/- 20MHz): a piezo which changes the length of the cavity by applying a mechanical strain on it;

- a slow actuator with a large range of correction (+/- 16GHz): a resistor used to modify the length of the optical path in the cavity by heating the crystal and changing its refractive index.
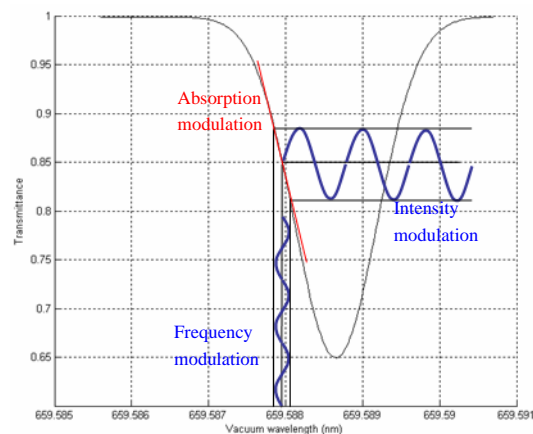

Figure 20   Principle of the Pound-Drever-Hall stabilization method.

The frequency stabilization system can be separated in two parts: an optical part mounted on a 75x90cm^2 breadboard and an electronic part whose elements are stored in the Metrology System Electronic cabinet. At Paranal the whole system will be located in the Storage Room

The whole optical part of the system in its basic configuration is presented in Figure 22. The power at the output of this the laser is splitted using a 25%/75% SM-PM fiber coupler from Canadian Instrumentation and Research Limited. The 75% output is connected to a SM-PM fiber which propagates the light to the heterodyne assembly. A SM-PM fiber is connected to the 25% output and guides the light to the focusing optics. The fiber is connected to a fiber aligner (New Focus 9091) and the light is focused using a lens (focal length 15.4mm) into a non linear crystal (Periodically Poled Lithium Niobate, HCPhotonics, 20x1x5mm^3) which doubles the frequency of the light (i.e divides the wavelength by two from 1.319μm to 659.5nm). The non linear crystal is held in a temperature controlled oven mounted on a New Focus (9071) translation stage. After the nonlinear crystal, the beam is collimated with a lens (focal length 40mm) and sent through an Electro-Optic Modulator (New Focus 4001M EOM) mounted on a New Focus stage (9071). The EOM modulates the phase with an amplitude of π at a frequency of 25MHz generating a frequency modulation of 80MHz amplitude at a frequency of 25MHz. The modulated beam propagates through a custom made cell containing iodine vapor. The I$_2$ cell is on a custom made mount. A dichroic high pass filter (Edmund Optics) separates the infrared light from the red light. After a folding mirror the visible beam is focused (60mm focal length lens) on an AC coupled detector (Analog Module 712-A2).

The signal coming from the detector is fed to the lock-in amplifier (Stanford Research Systems, Model SR844RF lock-in amplifier). The lock-in amplifier demodulates the signal using as phase reference a signal coming from the EOM driver (New Focus 3363B). The output of the lock-in amplifier is a voltage proportional to the rms amplitude of the

detector signal filtered at 25MHz with a 160Hz bandwidth. This voltage is the error signal of the control loop and is fed to the analog input board (VMIC VMIVME 3123) located in the LCU rack. The control loop runs on the **lprmls** LCU using TAC. Two correction signals are generated by the loop and are send respectively to the laser driver piezo input (labelled "fast input on the driver) and to the temperature input ("slow input") using two outputs of the digital to analog output board (MPV-955) located in the LCU rack. The laser driver applies then these signals on the two actuators which modify the laser optical frequency. The rest of the electronic is composed of two temperature controllers (Newport Omega CN77352-C4) for the crystal oven and the iodine cell, a 15V voltage generator for the detector.

7.2.2 Control architecture

The specificity of the control loop comes from the characteristics of the two actuators that can be used to correct for the frequency noise of the laser. Piezo tuning provides a fast correction with a high resolution but with a limited range of +/-20MHz which is usually exceeded when the laser is operated more than 30min. Temperature tuning offers a broad range of correction (several GHz) with a poor resolution and a small bandwidth. To correct the frequency noise the two actuators have to be used simultaneously despite their different scaling. The two loops work almost independently. The error signal seen by the temperature controller is just overestimated by adding the (converted) piezo correction signal. This is done to force the temperature loop to desaturate the piezo actuator. Such a scheme could create problem as the two loops, piezo loop and temperature loop, could compete against each other. Nevertheless in this case the scaling of the two loops is so different that the piezo loop has little effect on the temperature loop.
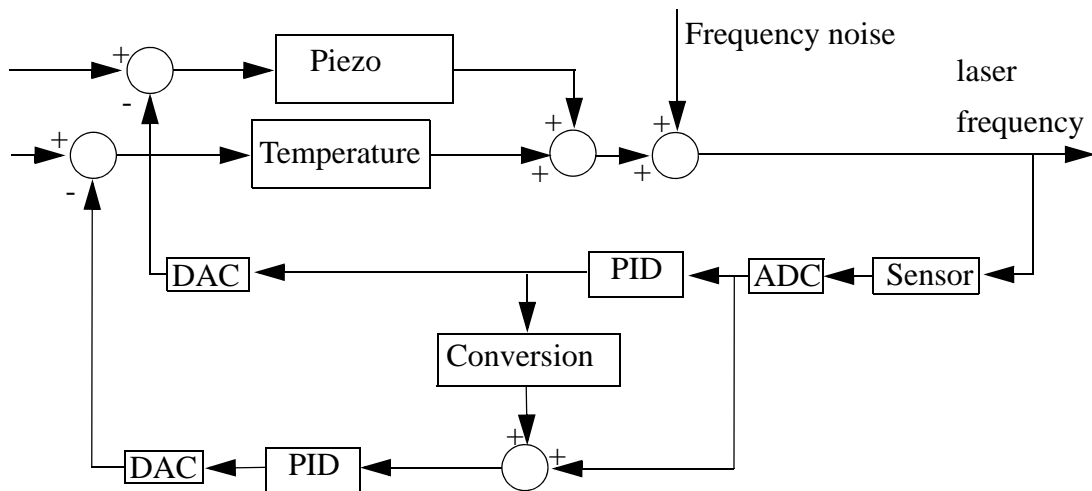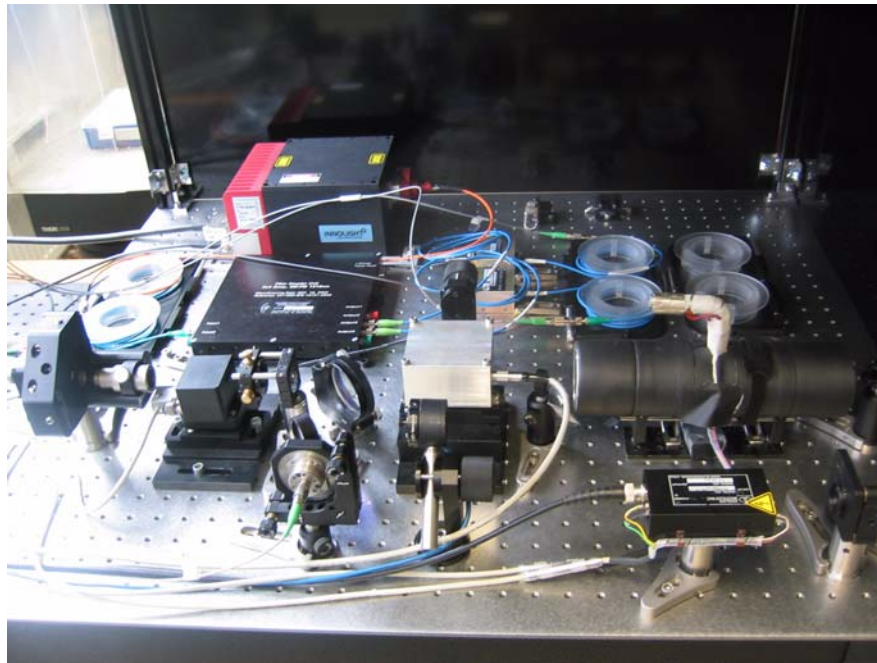

Figure 21   Design of the control loop.

Figure 22   Optical set-up of the PRIMA metrology laser absolute frequency stabilization system.

Figure 23   Light source system (laser stabilization, heterodyne assembly, control electronics) as implemented in the FTK test bed

7.2.3 Performance

The measured performance are detailed in RD 7 and illustrated in Fig. 24.

Over 30 min, the open loop frequency excursion is: $\sigma_f = 7.4$ MHz rms; $\Delta_f = 22$ MHz (P-V)

In the best case, the frequency excursion in closed loop was reduced to:

$$\sigma_f = 0.126 \text{ MHz rms}; \Delta_f = 0.892 \text{ MHz (P-V)}$$

In all cases, the specification of $\sigma_f = 2.27$ MHz rms was reached (i.e relative frequency error of $d\nu/\nu = 10^{-8}$).
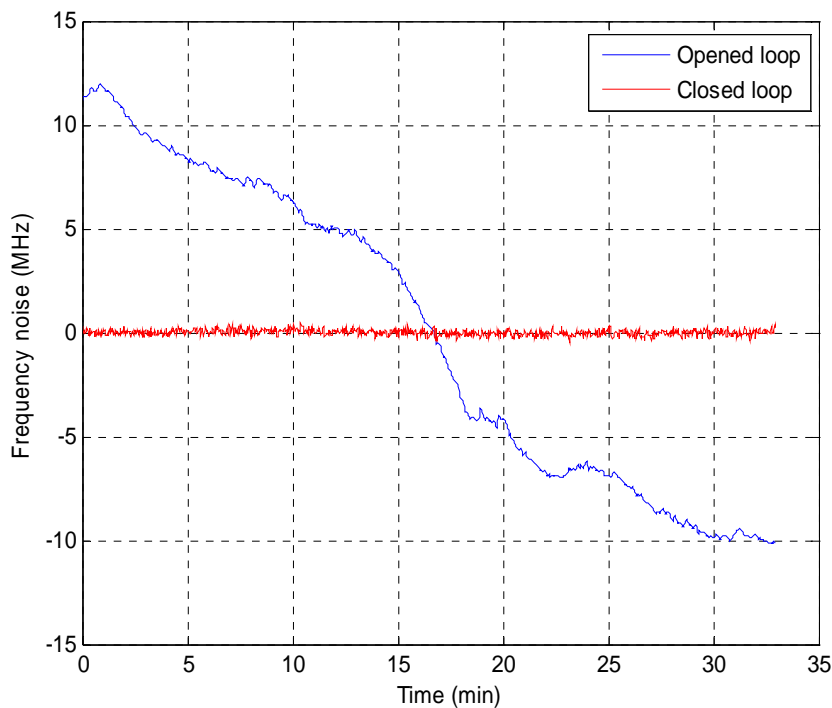
Figure 24   Performance of the frequency stabilization loop.Best case (see File 16_03_02 reported in table 14.1 of RD 7)

7.3   Heterodyne Assembly

7.3.1   Fiber Coupler Unit

The Fiber Coupler Unit splits the light of the linearly polarized Nd-Yag laser in four identical optical beams, while preserving the input linear polarization state. The four outputs are then connected to four different pigtailed acousto-optics modulators. The Fiber Coupler Unit provides 2 inputs and 4 outputs (2x4 array). One input will be used a spare input. Any remaining fiber end other than the 2 inputs and the 4 outputs are cleaved at an 8°angle to minimize the back reflections.The performance of the Fiber Coupler Unit is reported in Table 6. The Fiber Coupler unit includes a temperature controller to possibly optimize the throughput and the polarisation isolation performance.

Table 6   Specification for the Fiber Coupler Unit

Parameters	Specifications
Operating Wavelength	λ=1319nm
Polarisation state	Linear Isolation< -22dB[1]
Power Loss	0.1 dB per coupler
Splitting ratio tolerance	$\pm$3% (ratio 43/47) per coupler
Type of optical fibers	7/125/400/900 1310nm Fujikura Panda, SM13P Single mode and polarisation maintaining at λ=1319nm.

1. Cross coupling between the slow (p) and the fast (s) axis measured at 1 output of the 2x4 array, i.e it is the ratio of the "s" intensity over the "p" intensity assuming a perfect "p" input: 10log(s/p).

Two fiber coupling Units have been delivered by CIRL. The measured transmission is given in Table 7.

Table 7   Measured transmission of the Fiber Coupler Unit (including the adaptor losses)

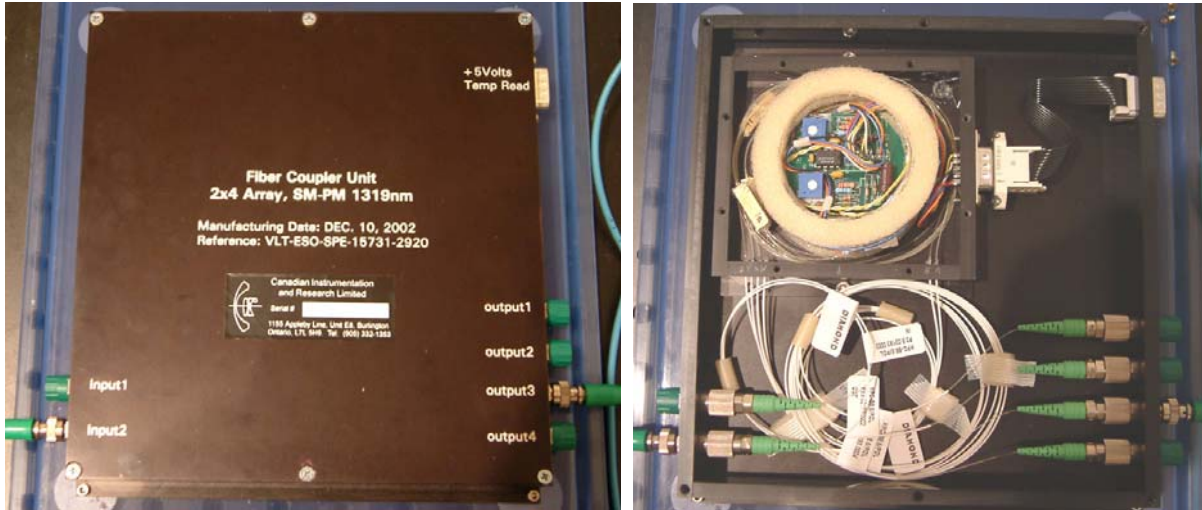| Parameters	% of input light at each output (input 1)
Serial 5173-1	Output 1: 21.7% Output 2: 22.2% Output 3: 24.3% Output 4: 23.9%
Serial 5173-2	Output 1: 21.9% Output 2: 23.5% Output 3: 22.4% Output 4: 23.6%

Figure 25   Fiber Coupler Unit of the metrology system (already delivered to ESO)

7.3.2   Pigtailed Acousto-Optics Modulators

We use the IntraAction FCM-1E6AP to frequency shift the laser beam by:

- Channel A (FSU A, Midi or Amber): +38.65MHz and +38MHz (heterodyne frequency of 650 kHz)
- Channel B (FSU B): -39.55MHz and -40MHz (heterodyne frequency of 450kHz)

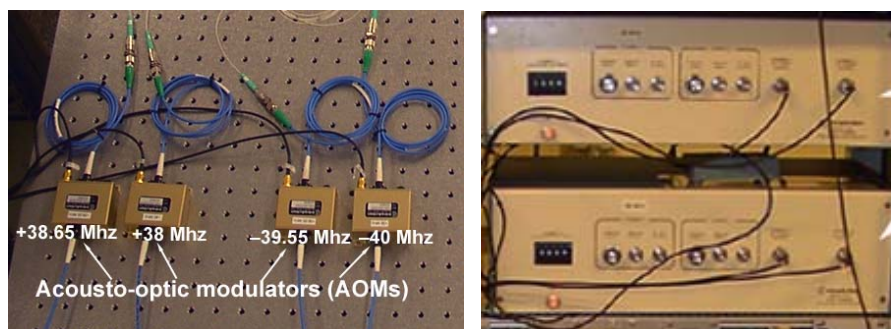The two drivers of the AOM's are stand-alone drivers (model DFE-404A4) which are installed inside the Metrology electronic Cabinet.

Figure 26   Pigtailed Acousto-optics Modulator and drivers, IntraAction FCM-40

The transmission of each AOM is specified better than 63% (without connector loss). It can be optimized to about 80% when providing the required frequency shift to the manufacturer.

8 Beam relay

The *Beam Relay* consists of four elements:

1/ "*Switchboard 1*" where the 4 outputs of the pigtailed AOM's are connected to the input fibers of the desired metrology channels (channel B: FSU#B; Channel A: Midi, Amber or FSU#A). This element is not remotely controlled. In a future phase, the switchboard could be replaced by optical switches for automatic routing. However, the impact of optical switches on power loss or de-polarizarion needs to be investigated. The Switchboard is simply an aluminium panel holding a set of single mode fiber adaptors (*MPC-S8.22-PM/6Kt.X (2mm key) from Diamond*) and inductive sensors. The inductive sensors are mounted close to each fiber connector such that the channels which are connected are known to the PRIMET control system, i.e which channel is operated in Channel A of the PRIMA Metrology (Midi Amber or FSU#A) and verify that Channel B is connected to the FSU#B channel.

2/ 8x *input fibers* which are connected from the "switchboard 1" to all metrology beam launchers. The characteristics of the fibers are:

- Number of fiber: 8
- Length: 35 m
- Type: 7/125/400/2800 1310nm Fujikura Panda, SM13P, Single Mode and Polarization Maintaining at λ=1319nm. possible supplier I.D.I.L, S.A
- Connectors: FC/APC connectors at both ends.HPC-S8.6-PM/K (2mm key). Key Aligned along the slow axis with a precision of +/- 0.8 deg. Supplier: Diamond GmbH

3/ 8x *output fibers* used to transfer the interferometric signals (probe and Reference) generated by the Beam Combiners to the inputs of the phase meter. The characteristics of the output fibers are:

- Number and length of the fibers: 8 fibers 35m long and 4 fibers 6m long
- Type: 62.5/125/400/2800, Multimode fiber for λ=1319nm.
- Connectors: FC/PC connectors at both ends.HPC-M0.66/K (2mm key). Supplier: Diamond GmbH

4/ "*Switchboard 2*" where all output fibers are connected. It is similar to "switchboard 1". Two pairs of fibers are routed to the phase meter. The "probe" and "ref" fibers of FSU#B are (always) connected to Channel B (450kHz) of the phase meter. The input of Channel A of the phase meter (650kHz) must be manually connected to the proper instrument channel. The status of the fiber connection is read by inductive sensors.

The input and output fibers will be permanently routed from the storage room to the interferometric laboratory, across the "feed through" of the storage room (see cabling in RD 13).
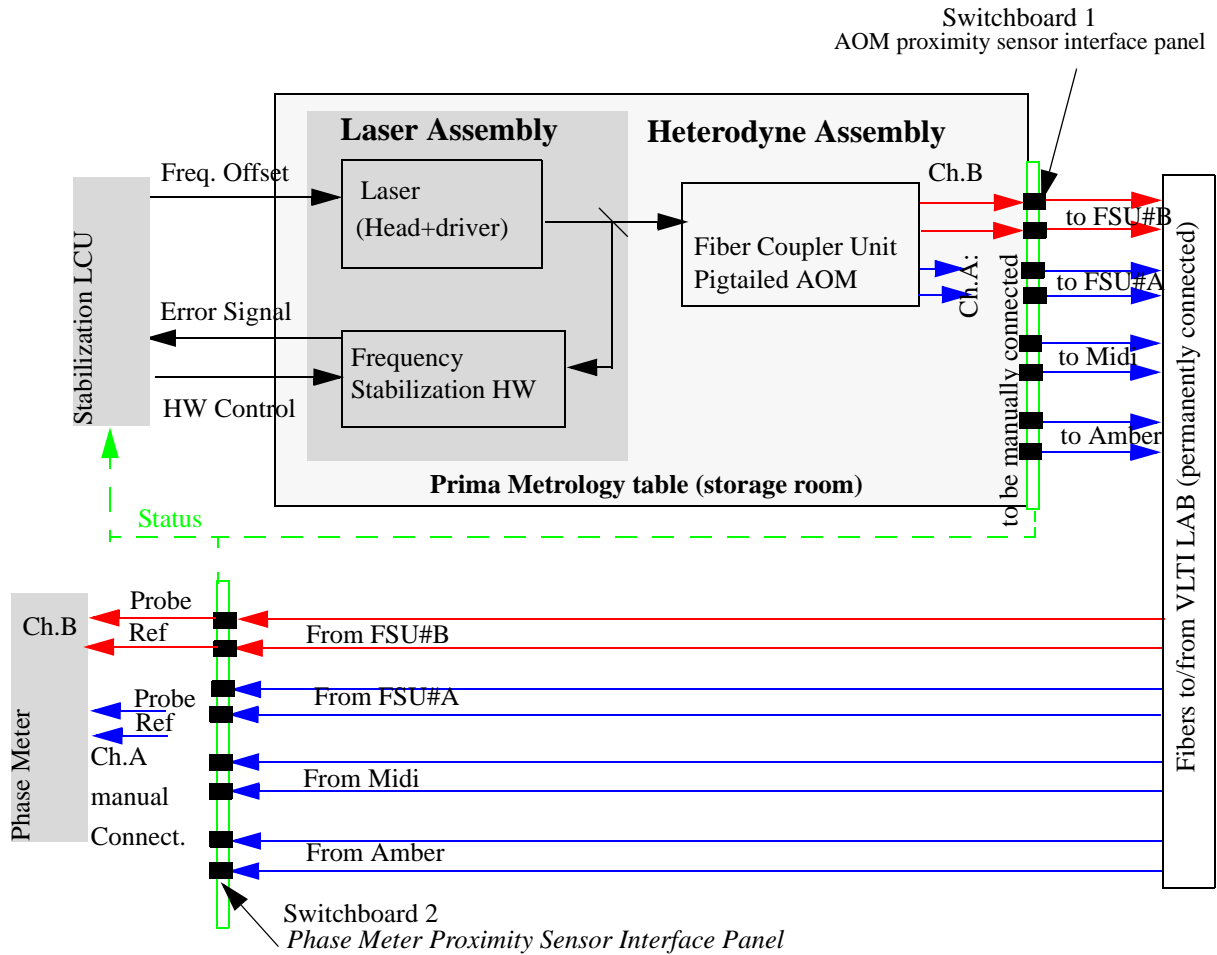
Figure 27   Beam relay (fiber routing using 2 "switchboards")

9   End Points (retro-reflectors)

The end-points are part of the design of the AT STS. The end points consists in a retro-reflector made of two spherical mirrors (RR2 and RR3) and a compensation plate (RR1) as shown in Fig. 28. The metrology beams coming from the laboratory along Channels A and B, assigned to the same interferometric arm, propagate up to the same STS (see Fig. 1). Both beams are transmitted through M9 and reflected back to themselves by the combination of RR1, RR2 and RR3. RR1 is a compensation plate, RR2 and RR3 are spherical mirrors. RR2 is located in a folded pupil plane of the telescope and RR3 in an image plane (conjugated with M10)

For each channel, the metrology beams and the stellar beams are superimposed and follow the same path from the laboratory up to the mirror M9[3]. For a single STS&Telescope, the non-common path error is the difference between 2 components:

---

3. the stellar beam and the metrology beam of a given channel have a common "chief ray" up to M9. Their physical size are different.

$$\varepsilon_{\text{sts\_tel 1}} = \varepsilon_{\text{m\_a/b}} - \varepsilon_{\text{s\_a/b}}$$

- $\varepsilon_{\text{m\_a/b}}$ represents the variation of OPD between metrology beam A and beam B from M9 to RR2.

- $\varepsilon_{\text{s\_a/b}}$ represents the variation of OPD between the stellar beam A and beam B from M9 to the primary mirror of the telescope. This should also be very small because even for a 1 arcmin_sky angular separation, both beams will have close footprints on all mirrors.

The global impact on the error on ΔL is given by $\varepsilon_{\text{sts\_tel 1}} - \varepsilon_{\text{sts\_tel2}}$

For each STS and telescope $\varepsilon_{\text{m\_a/b}}$ and $\varepsilon_{\text{s\_a/b}}$ should remain very small. Firstly both metrology beams will overlap on RR2 (pupil plane conjugated to the VLTI pupil). This means that the beams from M9 to RR3 are almost superimposed. Secondly, both stellar beams will have almost common footprints on all mirrors even for a 1 arcmin_sky angular separation. It is difficult to realistically estimate these quantities, and the final impact on ΔL. However, if we assume that the 4 contributions (in total) are uncorrelated, each of them should be limited to 2.5nm rms to limit the error on ΔL to 5nm rms.
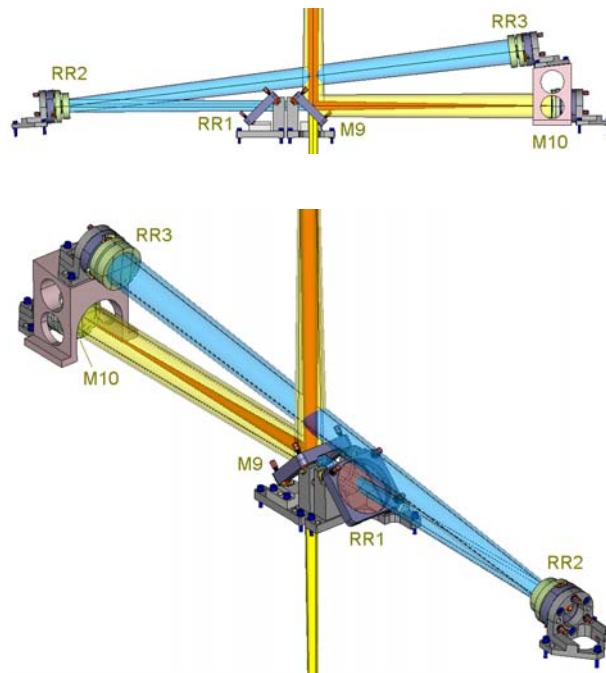

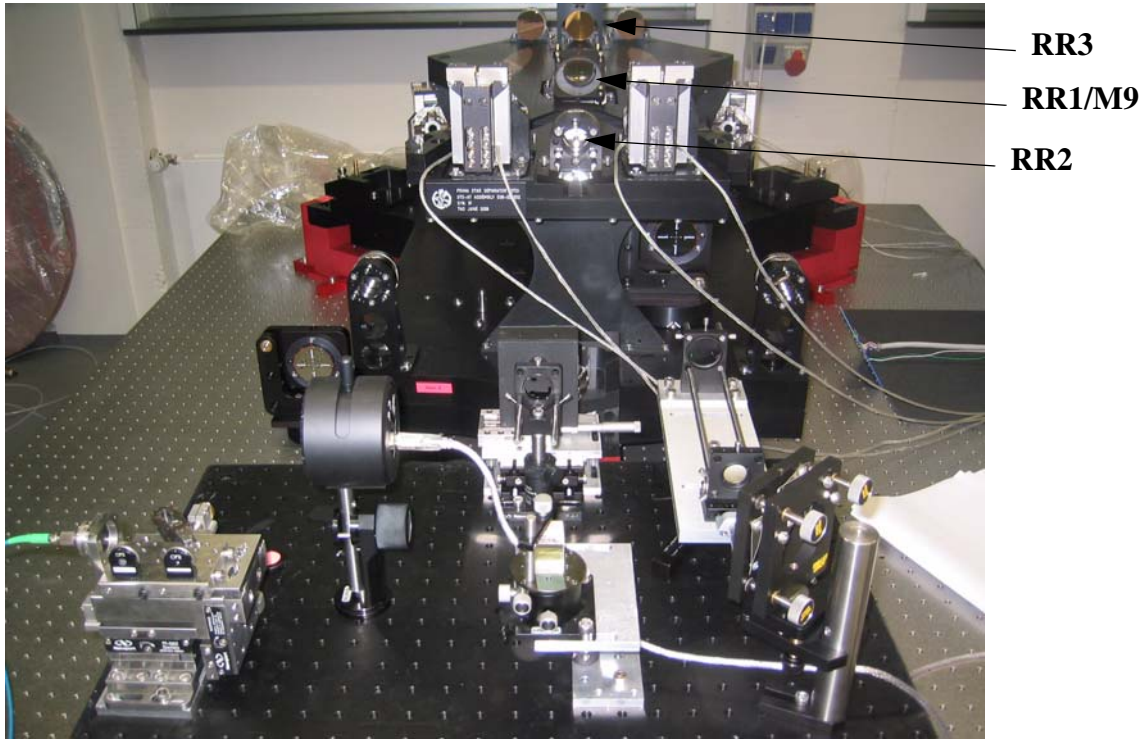*Figure 28   Design of the AT-STS end-points*

Figure 29   AT-STS during testing of the pupil tracker in Garching

10 Phase Meter

The Phase Meter is a standalone opto-electronic system mounted inside a VME crate which detects and process the interference signals generated by the two channels of the PRIMA Metrology system. Its role is to measure the phase difference between these signals, and make it available to the Metrology LCU.
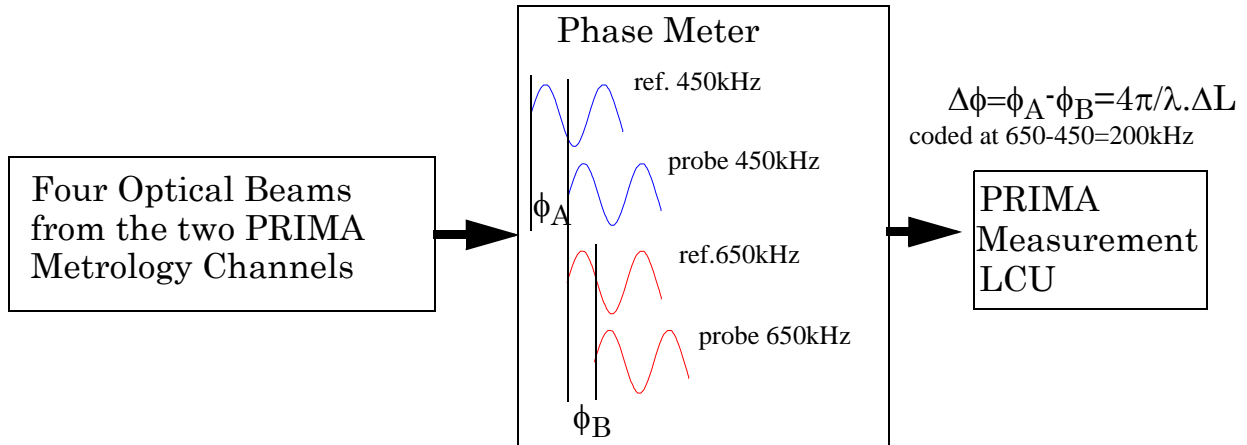
Figure 30   Functional sketch of the Phase meter

The Phase Meter as built status is documented in RD 11.

A phase shift of 2π corresponds to $\Delta L = \lambda/2 = 659.5$nm

In particular, the following performance applies to the photodetection & phase measurement chain:

- Resolution: $2\pi/1024$ rad (or $\Delta L = 0.64$ nm)
- Internal Sampling Frequency: $F_{s\_int} = 200$kHz
- Standard Deviation of the noise: < Resolution for an optical power >100nW per interferometric arm and a fringe visibility of V=70%
- Accuracy: $<2\pi/800$ rad (or $\Delta L = 0.8$ nm) for an optical Power of 20nW per interferometric arm and a fringe visibility of V=70% and a 50kHz Bandwidth.
- Bandwidth: B=110kHz for each interferometric channel (i.e ±55 kHz centered on their respective heterodyne frequency) and B=55 kHz for ΔL (i.e ±27.5 kHz centered on $F_{s\_int} = 200$kHz).

Upon reception of a trigger signal from the TIM board of the metrology LCU, the Phase Meter deliver at its P2 output the measured phase, $\Delta\phi$, as well as set of status data. The Phase Meter is connected via its P2 connector to a fast digital input board HPDI32 mounted on lprmac LCU. The role of this LCU is to process the data and status delivered by the Phase Meter. This includes the following tasks: average and convert ΔL in meters, write ΔL to the Reflective Memory Network as well as a status flag and a time step, and store engineering files.

The phase meter has an internal sampling frequency of 200kHz. However the TIM signal will have a maximum sampling of 8kHz. The phase delivered to the measurement LCU will actually be averaged on a minimum of 200/8=25 samples, thus reducing the measurement error.

Phase resolution / Range	
Differential phase	Resolution: $2\pi/1024$ or 0.6 nm
	Range: $2^{29} \cdot 659.5\,\text{nm}/1024 = 346\,\text{mm}$
Phase compensation	2π or 659.5 nm
	Range: $2^{24} \cdot 659.5\,\text{nm} = 11\,\text{m}$

Sampling frequency	
Internal (instantaneous phase)	200 kHz
External (accumulated phase)	0.36 Hz–15 kHz

Maximum OPL speed of DL and DDL ($v_{\text{OPLmax}} = \lambda\,\Delta v/2$)	
DL	
Specs: $450, 650\,\text{kHz} \pm 55\,\text{kHz}$	$\pm 36\,\text{mm/s}$
As built: $450, 650\,\text{kHz} \pm 75\,\text{kHz}$	$\pm 49\,\text{mm/s}$
DDL	
Specs: $200\,\text{kHz} \pm 27.5\,\text{kHz}$	$\pm 18\,\text{mm/s}$
As built: $200\,\text{kHz} \pm 34.5\,\text{kHz}$	$\pm 23\,\text{mm/s}$

Noise of the photodetectors
$-128\,\text{dBm/Hz}$ or $\text{NEP} = 0.14\,\text{pW}/\sqrt{\text{Hz}}$

Phase difference introduced by the bandpass filters (p. 23)
$< 0.42\,\text{deg}$ or $2\pi/857$ or 0.8 nm (peak).

Noise level of the digital phasemeter (p. 29)
(for 7 nW equivalent optical power, rms over 50 Hz–50 kHz.)
0.8 dig or $2\pi/1280$ or 0.5 nm.

Phase difference introduced by the movement of the DL	
(including the phase difference introduced by the bandpass filters, see above)	
Phasemeter "Spare 1"	$2\pi/256$ or 2.6 nm (limited by the set-up)
Phasemeter "Spare 2" $\sigma_1=$	$2\pi/426$ or 1.5 nm

Accuracy
$\sigma_2 = 2\pi/800$ or 0.8 nm (rms) over OPL = 180 mm.

Figure 31   Phase meter performance summary
The total error is sqrt($\sigma_1{}^2 + \sigma_2{}^2$)=1.7nm rms

11 Control Hardware

The PRIMET control hardware is distributed in 3 electronics cabinets as shown in Fig. 32 to Fig. 34. These cabinets will be located inside the storage room (IC104). A detailed description of all the control hardware, including cabling, can be found in RD 13.
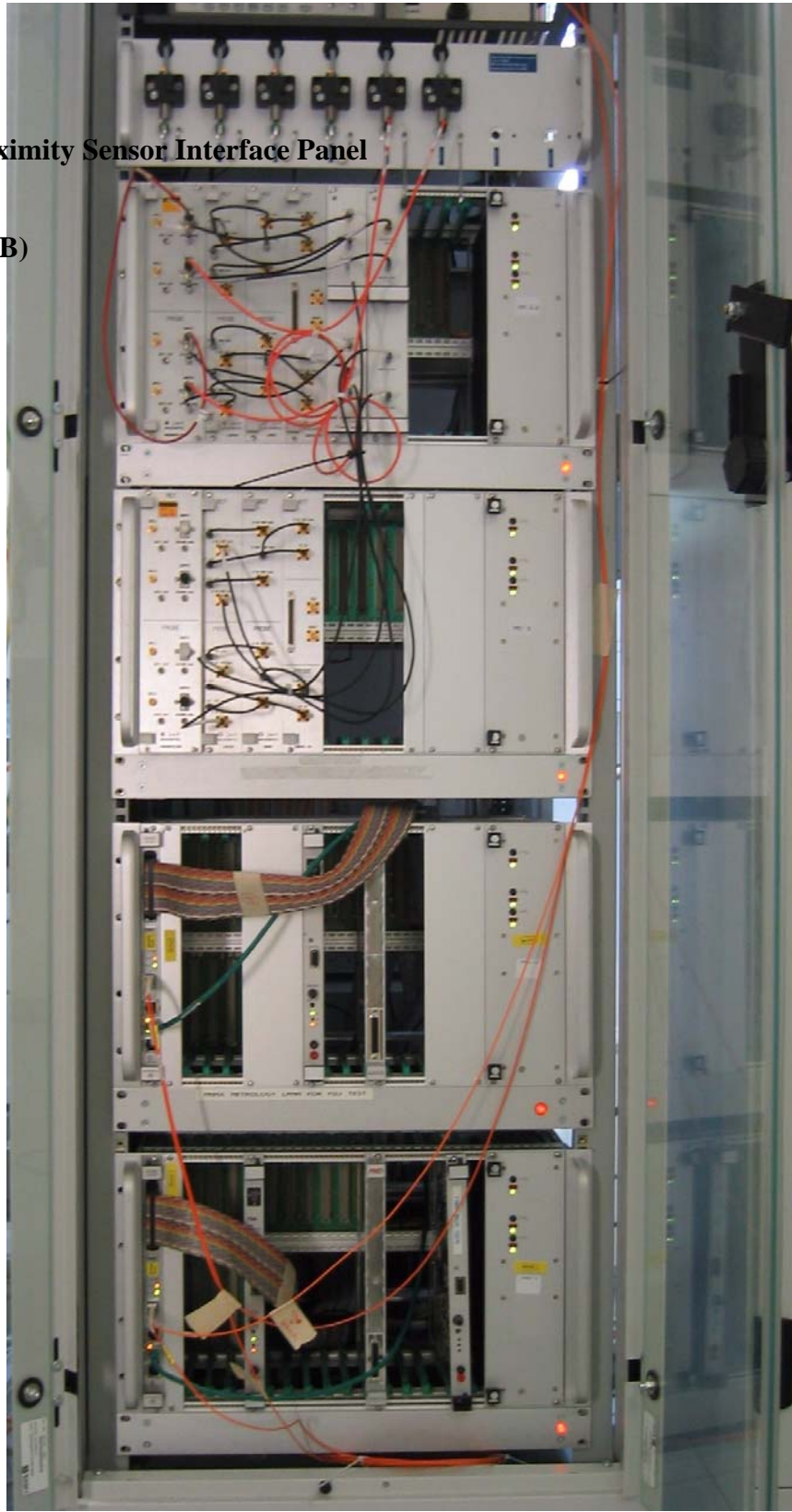

Figure 32   Metrology Cabinet 1 during testing in Garching

Phase Meter Proximity Sensor Interface Panel

Phase Meter (A-B)

Phase Meter (-B)

lprmac

lprma2

Figure 33   Metrology Cabinet 2 during testing in Garching

Figure 34   Metrology Cabinet 3, hosting the laser driver

12 Control Software

The PRIMA control software is split into 4 elements:

A workstation process, PMCS, controlling all PRIMET sub-systems and 3 LCU software modules:

- pmlss: it controls the laser power (laser head, AOM transmission) as well all frequency stabilization. The associated engineering GUI is "pmlssGui ".

- pmpsd: controls the pupil tracking loop, including an automatic beam search. The associated engineering GUI is "pmpsdGui "

- pmcs: reads the phase meters data, analyses status data and write them on the RMN. The associated engineering GUI is "pmacqGUI".

The algorithms, data handling and operation scenario are described in RD 16, RD 17.

The software detailed implementation is described in RD 15 and the associated software user manual is described in RD 18
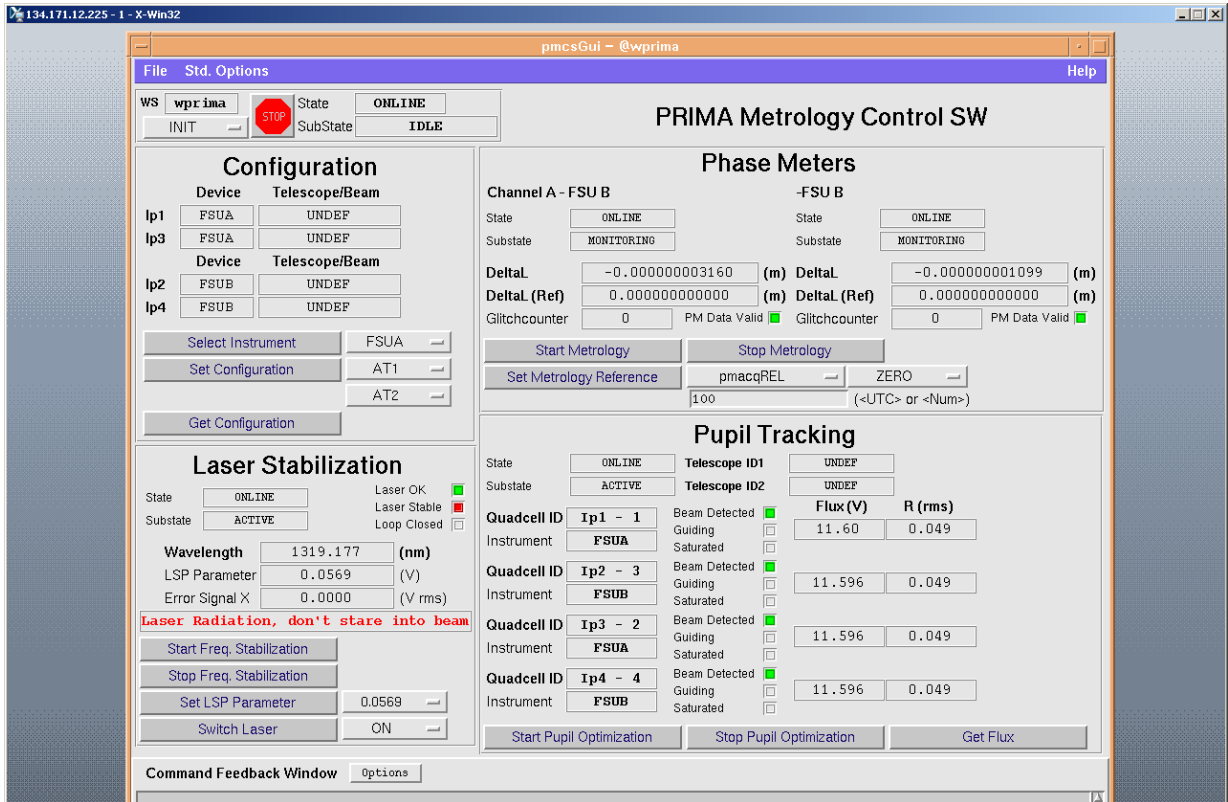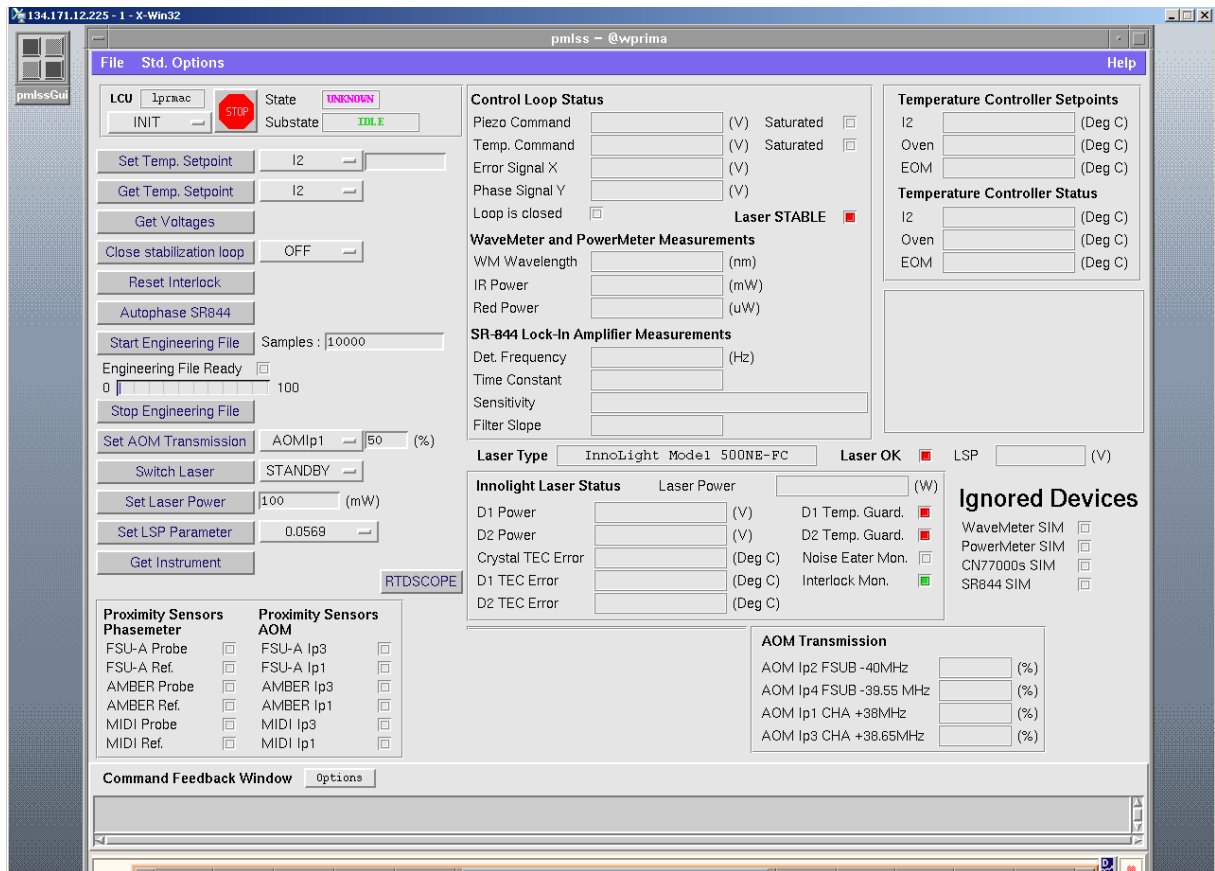
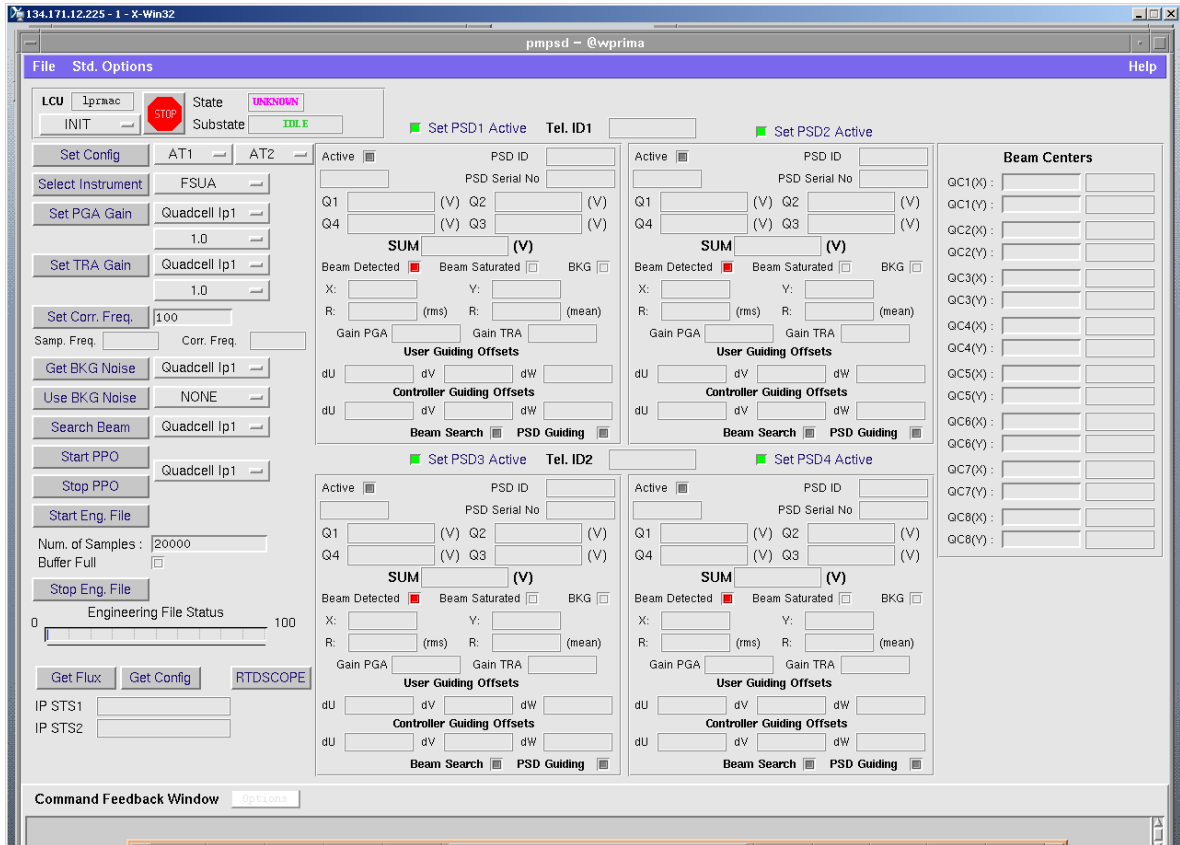*Figure 35   pmcsGui*

Figure 36   pmlssGui

Figure 37   pmpsdGui
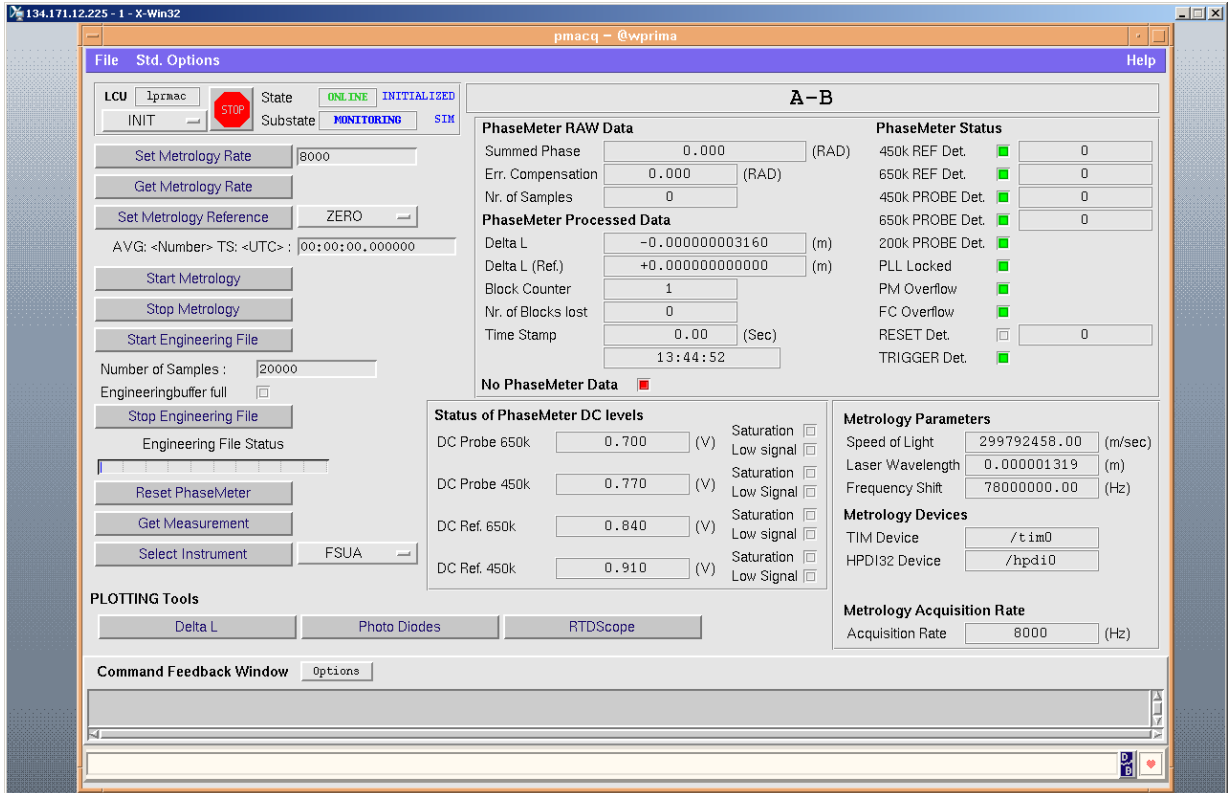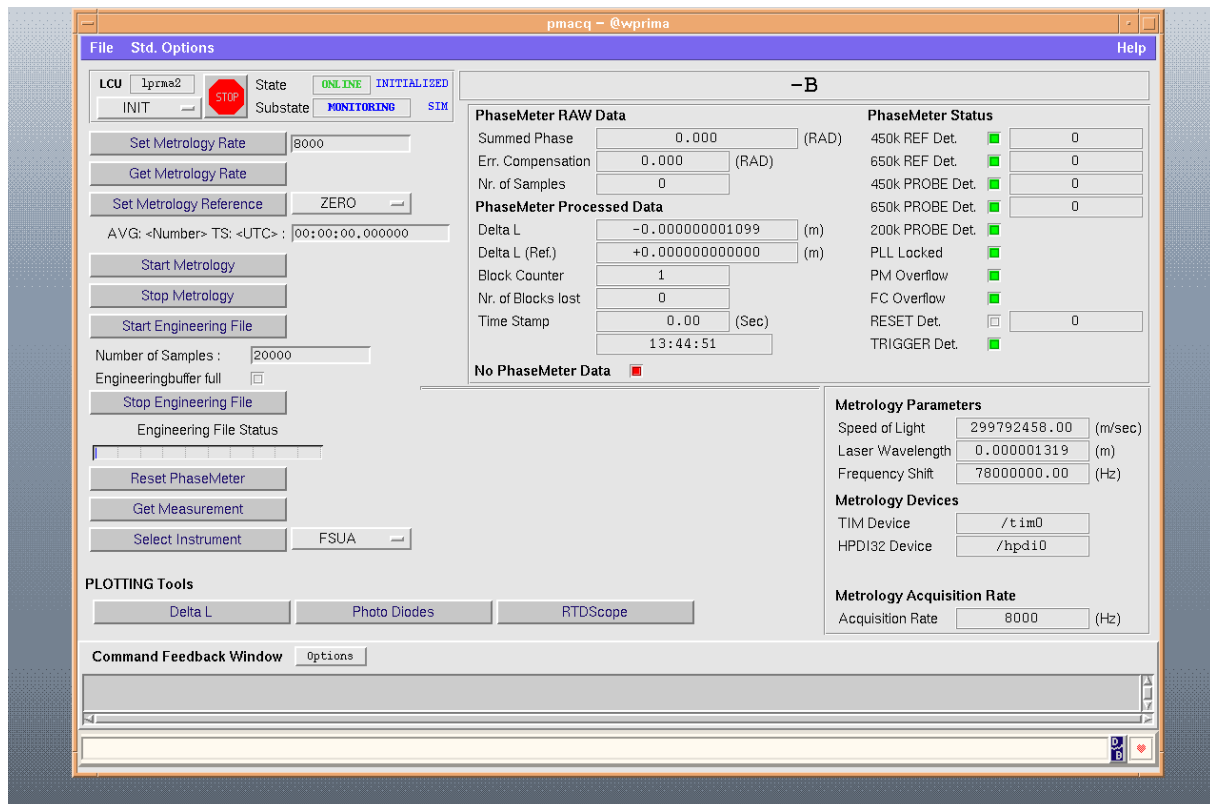
Figure 38   pmacqGui

Figure 39   pmacqGui for lprma2

13 Safety and reliability

The PRIMET safety and reliability aspects are described in RD 4.

PRIMET is equipped with a safety interlock system, RD 14, allowing a safe access in the VLTI storage room, in the VLTI laboratory where the laser is located. The entrance of the G2 maintenance station as well as the UT coude room will also be quipped with a safety interlock. Laser goggles will be available in all area where the laser beam propagates.

14 Performance Summary and verification matrix

The measured performance of the PRIMA metrology are highlighted herebelow.

Table 8 shows that the error on ΔL is limited to 5.35 nm rms but excluding the contribution of the non-common optical path. At this stage it is not possible to give a quantitative estimate of this contribution.

Table 9 summarizes the system performance.

Table 8   Error budget for ΔL

Source of error	Value	Reference
Laser Head		
Frequency stability 10^{-8} (for 0.6 nm rms ΔL= 60 mm) and Absolute accuracy of the Laser wavelength: 10^{-8} (0.6 nm rms for ΔL= 60 mm)	sqrt(2).0.6= 0.85 nm rms	section 7.2, RD 7,
Electronics		
Heterodyne assembly, Fiber relay, Phase meter	1.7 nm rms[1]	section 10, RD 11
Optical Configuration		
Polarization Cross-talks (3.5 nm 0-Pk for each channel, 7nm 0-Pk for the 2 PRIMET channels))	5 nm rms[2]	RD 5

Non-common optical path:
        FSU Channel
        STS
	~nm level (Δbeam footprint)
	TBC(ΔL M9-M2)
		"by design"
		section 9

TOTAL (uncorrelated without STS contribution)	**5.35 nm rms**	

1. based on section 10, Figure 31.
2. 3.5 nm 0-Pk for each channel, i.e 7nm 0-Pk for the 2 PRIMET channels. Considering that the polarization cross-talk error is a sine with a period of 1 λ , the rms is 7/sqrt(2)=5 nm

Table 9   PRIMA Metrology System performance and verification matrix

Parameters	Value	Verification
ΔL Noise	0.5 nm	in spec.
ΔL Resolution	0.6 nm	in spec.
ΔL Accuracy	5.35 nm ([1])	"small" discrepancy
Maximum ΔL speed	$d\Delta L/dt <+/- 27$ mm.s^{-1}	in spec.
Sampling frequency	8kHz ([2])	in spec.
ΔL Range (before wrapping)	346 mm	in spec.
Operating Wavelength	$\lambda=1319$nm	in spec.
Laser Frequency Stabilization	$d\nu/\nu<10^{-8}$	in spec.
Straylight on the FSU detector	2.7 e$^-$ ([3])	in spec.
Pupil Tracking residuals	10% of the beam radius ([4])	in spec.

1. excluding non-common path errors
2. The maximum sampling frequency of ΔL provided by the phase meter is 15kHz. However, the metrology control software uses a maximum value of 8kHz.
3. this value is 1000 less than the thermal background
4. this corresponds to 100 μm for a 1mm beam radius

15 Appendix

15.1 Estimation of ΔL by beam swapping

<u>Before beam swapping:</u>

S_1 observed on Beam combiner A through channel A

S_2 observed on Beam combiner B through channel B

$OPD_{S1/A} = B. S_1 + L_A$
$OPD_{S2/B} = B. S_2 + L_B$

<u>After beam swapping:</u>

S_2 observed on Beam combiner A through channel A

S_1 observed on Beam combiner B through channel B

$OPD_{S2/A} = B. S_2 + L_A$
$OPD_{S1/B} = B. S_1 + L_B$

Therefore: $(OPD_{S1/A} - OPD_{S2/B}) - (OPD_{S1/B} - OPD_{S2/A}) = (L_A - L_B) - (L_B - L_A) = 2.\Delta L$